uc3m | Universidad Carlos III de Madrid

DEPARTMENT OF THERMAL AND FLUID ENGINEERING

BACHELOR'S DEGREE IN ENERGY ENGINEERING
2016-2017

Bachelor's Thesis

EXPERIMENTAL STUDY OF HEAT TRANSFER IN MOLTEN SALTS

Madrid, 4th of July of 2017.

Author: Pedro Moreno Martínez.

Tutors: Carolina Marugán Cruz.

María Fernández Torrijos.

ABSTRACT

Solar energy is one of the fastest growing technologies of our time, with the benefits of reducing the dependence from fossil fuels and produce clean and sustainable energy. The experiment that this report describes is focused on the thermal solar power generation and specifically in the receiver of the tower solar power plants.

This present Project has the objective of study the heat transfer inside the tubes of a concentrated solar receiver of tower type with molten salts as heat transfer fluid.

Several experiments have been performed in order to have the best possible estimation and this work summarizes the tasks done previous to the start of the experiments as well as the results obtained and the conclusions reached.
The working conditions of the experiments simulate the real performance of existing solar thermal power plants referred to the temperature of the salts and its mass flow through the tube.
The calculations done during this project have been performed with the help of the software Matlab R2012b while the acquisition of the data corresponds to the software LabVIEW.

This report in englobed in a bigger project founded by the government of Spain with the objective of improve the existent receivers of the thermal solar power plants.
After obtaining the results a critical comment is performed and the future perspectives are explained.

The objectives of this final bachelor project have been achieved with better results than the expected at the beginning, a fact that allows to think positive about obtaining the targets established by the main researchers of the installation in the future.

INDEX

FIGURE INDEX

TABLE INDEX

PRESENTATION AND MOTIVATION

This Bachelor Final Project is focused on an experiment held in the University Carlos III of Madrid by the department of thermal and fluid engineering with the name of “Study and design of new central solar receivers”. My contribution to this project is mainly the help for starting the experiment and analyzed the initial results. This university experiment is inside the National Plan document and is subsidized by the Spanish government with the ambition of learning more about this growing technology.

Solar thermal power plants are increasing their presence around the world and Spain is one of the biggest energy producers using this energy source, but for this technology to become really attractive in economic terms a lot of factors must be improved. The final scope of this subsidized project is to improve the design of the central receivers and by this optimize the thermal efficiency, avoid thermal fatigues, and increase the maximum working temperature of the plant.

My personal motivation to start this project is the need of improvement of this innovative power plants and my desires for learning more about a type of energy that in the future will substantially change the way society is able to interact with the environment, eliminating the harmful CO2 emissions from the electricity production.

OBJECTIVES OF THE PROJECT

This final project focusses its attention in the commissioning of the experiment for achieving relevant data about the functioning of the installation. This data will be used to improve the experiment towards a closer simulation of a commercial concentrated solar power (CSP) plant. The final goal consists on showing the results obtained from the data achieved during several experiments. Also, this final project is performed expecting to be a guidance for future researchers in the solar thermal field and specifically in the installation under study.

In this context, we can summarize as main objectives the following:

1. **Achieve enough knowledge about thermal power plants for understanding and be able to manage the experimental project.**

   For this objective, it was mandatory to read the previous bibliography about previous researchers in the central receiver field.

2. **Commission of the experiment for the data collection.**

   The commissioning of the experiment has been one of the biggest step due to the troubles appeared related with some parts of the installation.

3. **Once the results are obtained, be able to calculate relevant values for understanding better the functioning of a real plant.**
   Calculations about the heat transfer inside of the tubes have been performed.

4. **Critically review the values obtained**
   Critical study of the temperature distributions has been performed.

PROJECT STEPS

For achieving the previous explained goals, we can divide the work performed on different phases:

1. Reading and understanding previous works related to experiments that have tried similar procedures.

2. Preparation of the experimental simulation. In which helping to commission the experiment has helped me to understand it.

3. Acquisition of the experimental data with the help of LabVIEW software and its processing by means of Matlab R2012b. Once the code has been programed different changes can be applied in a simple manner achieving a real comparison between the obtained results.

4. Evaluation of the results obtained and comparison to the ones expected. Microsoft Excel has been use for facilitating the reading and understanding of some results.

5. Composition of the report.

1. INTRODUCTION

Solar energy is viewed as one of the most promising technology and is already advancing in the energy market reducing the dependence of fossil energy sources and the need of third countries energy supplies. Spain is recognized internationally by its efforts on the solar energy field and in the research of improvement on solar concentrating power. This work is embedded in one of these research experiments.

For starting this final project, firstly the actual energy situation will be presented, followed by the push from the governments toward a cleaner energy production, which will be justified by the introduction of the world compromises. Then the solar energy sector will be covered with special attention to the solar thermal type and, for ending this brief introduction, the Spanish advances in the technology will be summarized.

1.1. ENERGY SITUATION

The world energy resources are changing rapidly. During the past years, we have seen a tangible variation in the global energy market. The countries are betting hard in the renewable sector changing the primary energy consumption ratios by diversifying their installed power and by this, growing the evolution of smart grids and their independency from other not controlled sources.

On the following diagrams, we can see how the energy sources have diversified the Spanish energy mix in the past years, changing from a few energy sources to the actual situation.

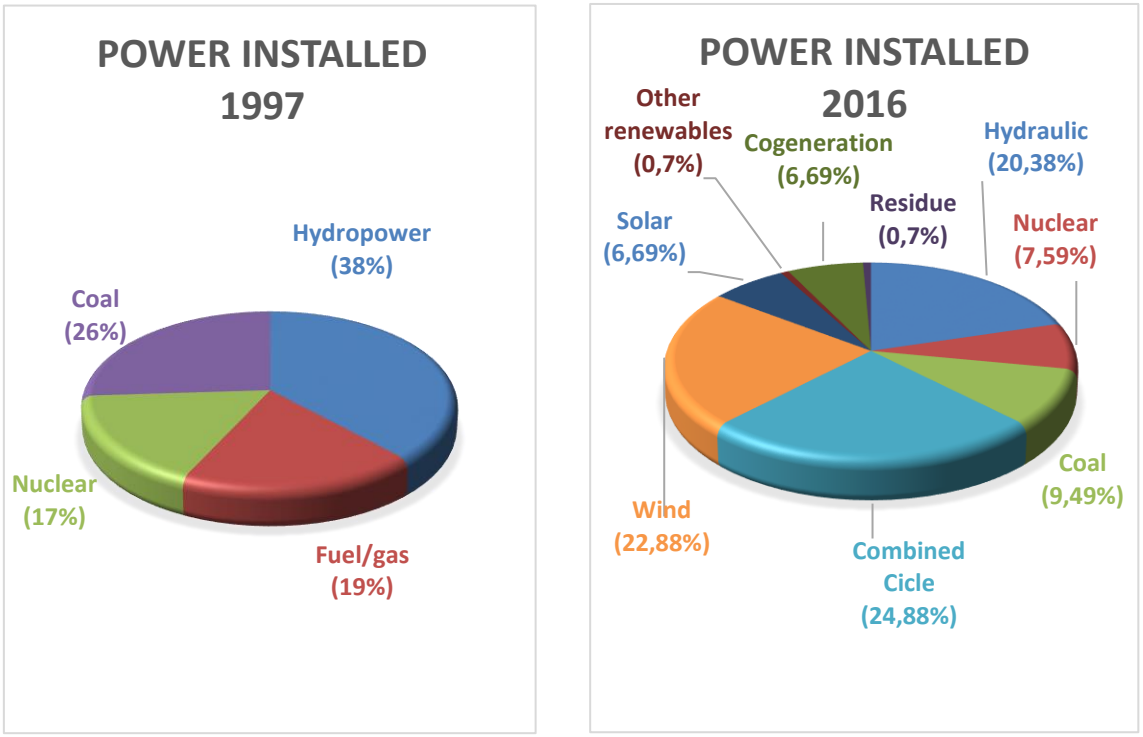

a) *b)*

Figure 1: a) Percentage of power installed in 1997 [1]. b)Percentage of power installed in 2016 [2].

The transition shown in Figure 1 is unstoppable, though the crisis has made the change slower the objective for the future with respect to CO2 emissions and the concerns of running out of the reserves of conventional energy resources will keep changing the energy mix until it is completely sustainable. As we can see on the previous graph the renewables energies correspond nowadays a big percentage of the installed power but they keep having the drawback of its intermittence. This fact is helping to develop new ideas and ways of improving the existing capacity, on this matter the solar thermal power plants have a big opportunity for becoming one of the agents of the energy transition.

1.1.1. ENERGY DEMAND

The world energy demand has constantly grown throughout the years, this trend is set to continue due to the increasing population and the push from the developing countries. The fact that most of these developing countries have optimal solar conditions could help to increase the solar power plants use.

Energy consumption is increasing constantly during the past years as we can see on the following graph:

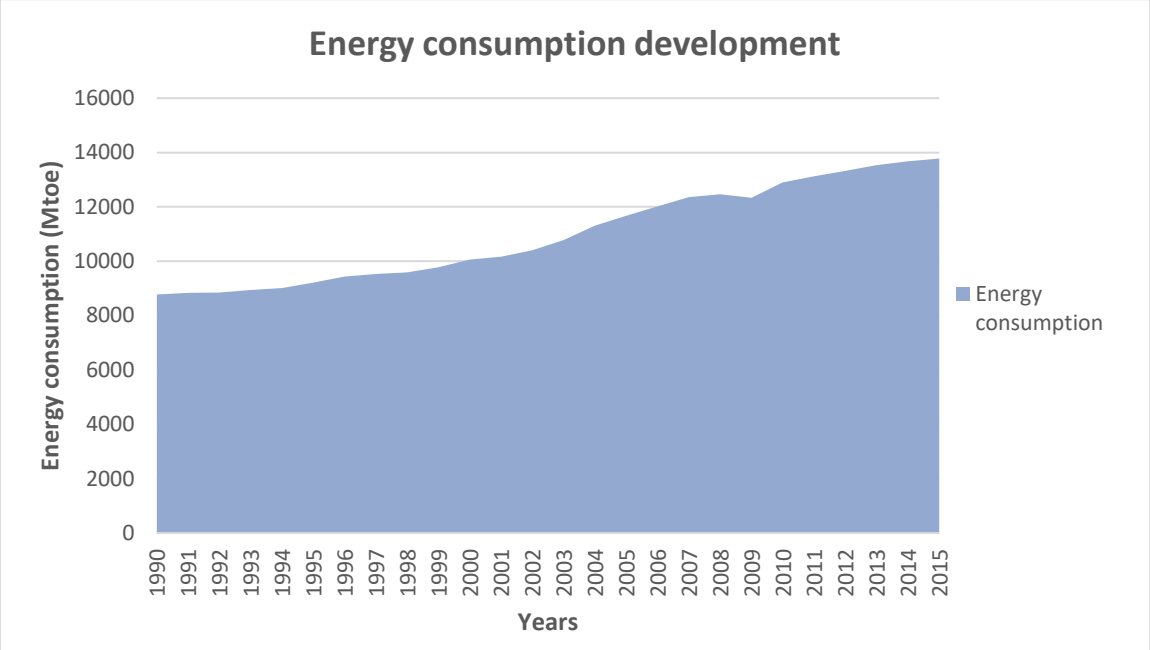

Figure 2: Energy consumption pattern [3].

The previsions for the energy consumption continue with the already shown trend of significant growth. The U.S Energy Information Administration estimated that the worldwide energy demand will suffer a 48% increase from 2012 to 2040 with renewable energy being the fastest growing source of energy followed by nuclear energy but with the maintenance of fossil fuels, such as liquid fuels, natural gas, and coal, accounting for 78% of the world energy consumption [4].

Actual trends in energy production and consumption are unsustainable economically, environmentally, and socially as the International Energy Agency (IEA) explains in several of their roadmaps. These reports are focused on growing clean energy technologies in order to give to the international community a path towards applying policies and financial support [5].

The push towards renewable energies is not only a way of reducing CO2 emissions but also is important due to the depletion of the conventional energy sources. As BP

Statistical Review of World Energy of 2015 shows, the known sources of conventional energy at the rate we consume them won't last much longer. Coal could last 114 more years with the actual reserves, while for natural gas there will be sufficient reserves to meet 52,8 years of current production. For the oil the previsions are even worse with an expectation to last 50,7 more years at current consumption rate [6].

The energy problem is deeper in undeveloped countries which do not have the capacity to supply energy to sectors of their population. With the relatively new solar technologies, countries with good predisposition as the ones situated in the show call solar belt, which contain approximately 78% of the world population [7], will be able to use the power of the sun in their benefit.

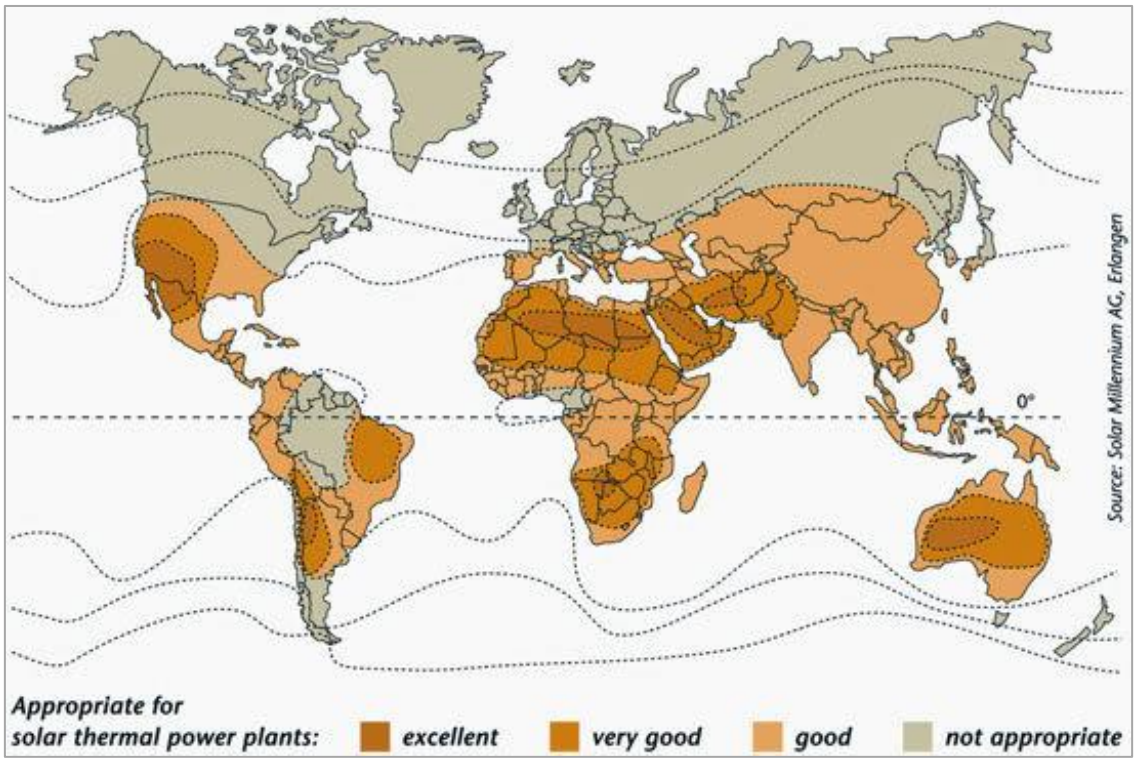

Figure 3: Solar belt.

Benefits from sun power deployment can be summarized as:

- Reduction of harmful CO2 emissions.
- Good system for isolated regions.
- Use of degradation land.
- The availability of solar energy reduces the dependency of other countries for the supply of energy.
- Increase of employment.

1.1.2. ENERGY LEGISLATION

The climate change is a problem that affects us all, nowadays we are more conscious of the risk that the human activities will imply for the future generations and luckily there are movements in order to stop the climate change from being an irreversible process.

First, we must explain the initiatives that inspired this project by going back to how European policies started to take consciences about the need of sustainable development in relation to the climate change that was starting to be noticed in the last decades of the past century.

In 1987 UN World Commission on environment and development (WCED) stablished that sustainable development could be obtained by providing the energy requirements of the present without compromising the ability of future generations to meet their own needs, a statement that could be seen as the reference for the next years regulation [8].

A year after, the Intergovernmental panel on climate change (IPCC) was created, this organism is the international body for assessing the science related to climate change. It provides policymakers with regular assessments of the scientific basis of climate change, its impacts and future risks, and options for adapting and mitigation [9] .This group published two years later their first evaluation in which 400 scientists reported the reality of global warming.

This mentioned report drove the governments toward the creation of the UN Framework Convention on Climate Change (FCCC) which entered into force in 1994 and was able to bound member states to act in the interests of human safety even in the face of scientific uncertainty. Today it has near universal membership [10].

This FCCC was the base for the well-known Kyoto Protocol of 1997 where the industrialized countries promised a reduction of greenhouse gases emissions.

On the next picture, we can appreciate how the countries respond to the Kyoto Protocol at its beginning.

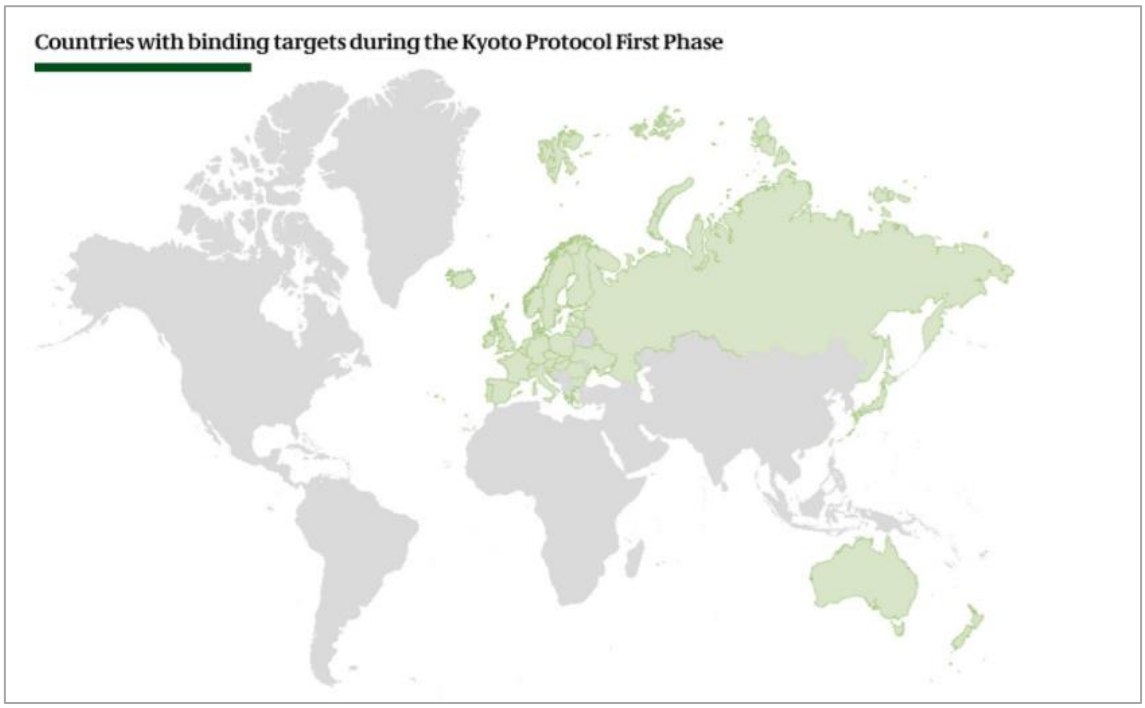

Figure 4: Countries response to the Kyoto Protocol [11].

In respect to Spain, the government compromised to produce only 15% more of the emissions of the base year (1990/1995) for the average of the years 2008-2012. This target was not achieved by means of reducing the CO_2 emissions but paying rights for the excess of CO_2 emitted.

In 2008, after eleven months of negotiation, the European parliament approved the climate change package 2013-2020 which tried to ensure that the European Union will accomplish the objective of a 20% reduction in greenhouse emissions, a 20% energy consumption from renewable energies and a 20% improvement in energy efficiency by 2020, these objectives are also known as the 20-20-20 targets. With this, Europe was again leading the work against climate change [12].

After this agreement, the countries started to work on a plan that could substitute the Kyoto Protocol that was going to finalized in 2012, for this purpose the conference of Copenhagen was held in 2009, where the most positive points achieved were the announcement of the necessity of limiting the rising global temperature level to 2ºC and the compromise of the develop countries of providing 30 thousand million $ with the objective of reducing the climate change.

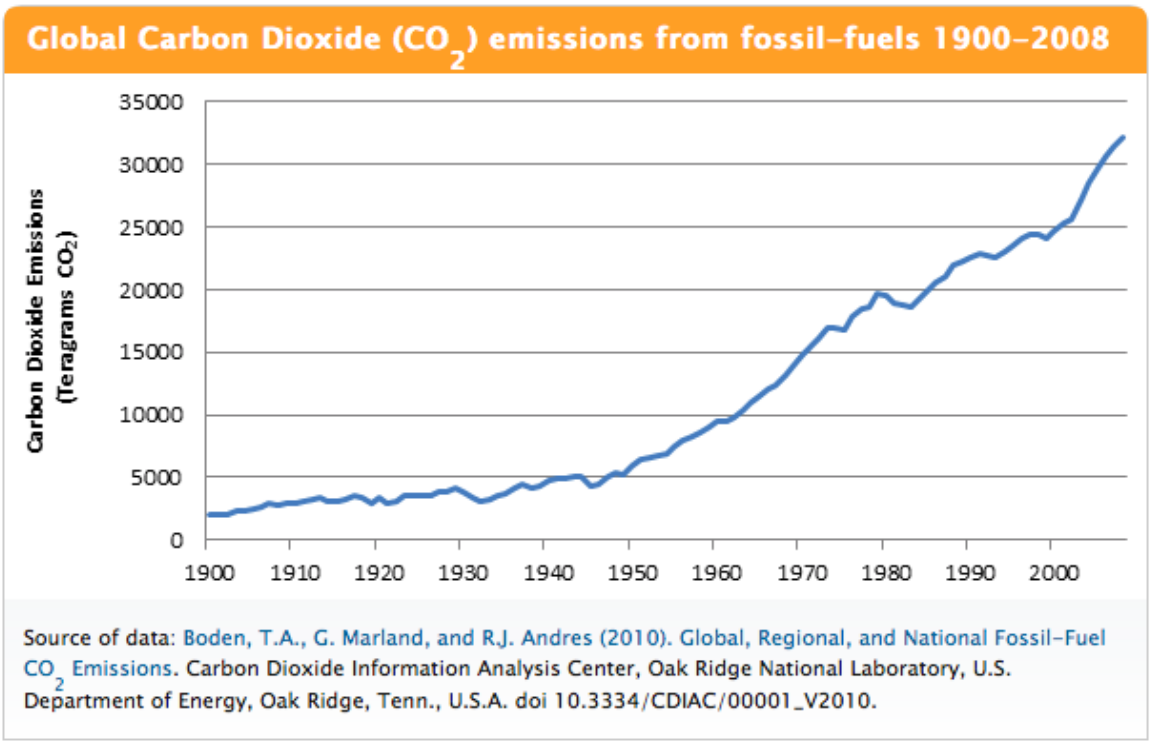

Figure 5: CO2 emissions development.

As we can see on the previous graph the global CO2 emissions where rising with higher slope than before during the 1900/2008 period which meant that more measures where needed.

The most recent step was taken by 195 nations in the conference of Paris in 2015 where an agreement for limiting global warming under 2°C was achieved and by proposing efforts for reaching a limiting temperature of 1.5°C in order to have a safer position against the global warming effects.

This final agreement covers important points such as:

- Reduction of the greenhouse emissions.
- A system to record the climate action.
- Strengthen the countries against the climate changes effects.
- Reinforce the ability of the countries to recover from the effects of climate change.
- Financial support.

[13]

Also, we must mention that the European parliament in the European council of October 2014 approved the 2030 framework where the different nations accepted the following objectives:

- 40% reduction of greenhouse emissions in comparison to the levels of 1990.
- 27% share of renewable energies in the final consumption.
- 27% improvement of the energy efficiency.
- 15% electricity interconnections.

And for the 2050 with a low carbon policy economy without binding agreements but with the main goal of achieving a level of 80% reduction of the emissions of 1990. [14]

After this summary of the European policies we can understand better the efforts of our government to improve one of the technologies that directly reduces the greenhouse gases emissions by cutting down the needs of producing energy from contaminant sources. The subsidize of this experiment is a clear example of a policy towards reaching the objectives that Europe and Spain have compromised to fulfill during the following years.

1.2. SOLAR ENERGY

Currently we can divide the solar energy environment in two main categories differentiated in how they transform the solar radiation to electricity:

- Photoelectric solar energy (PV).
- Concentrated solar power (CSP).

In 90 minutes, the earth receives enough solar energy for fulfilling the entire planet energy needs of one year. Solar energy is suffering a rapid development from its beginning in the mid-2000s due mainly to the policies of developed countries, the rising prices of fossil fuels, and the need of having additional energy supplies. This development of the industry is contributing directly to the reduction of production costs and the increase of efficiency. This is especially true for the photovoltaic systems, but also the concentrating solar power is growing. On the following figures, we can see this development:

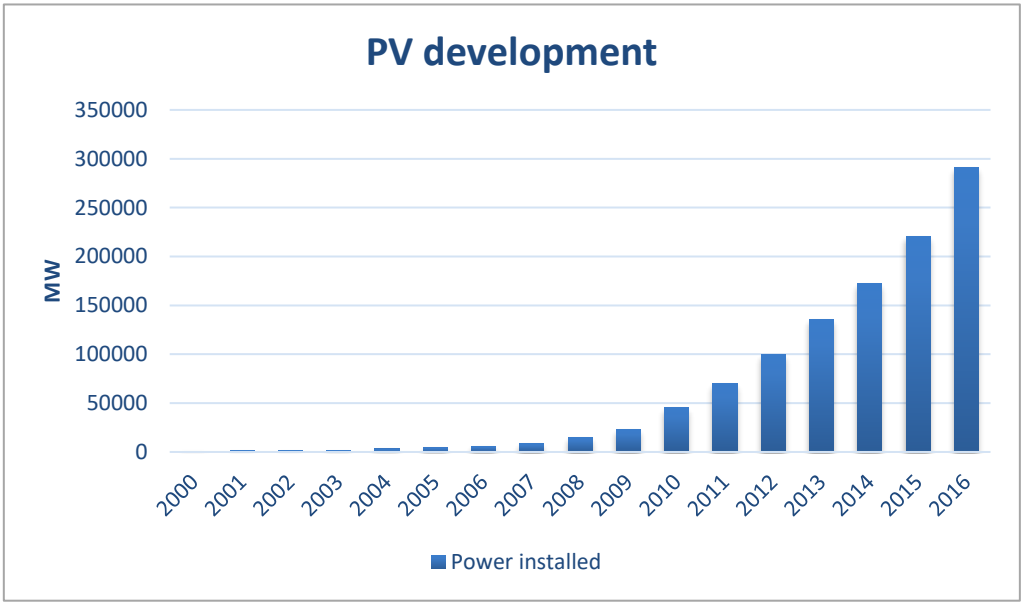

Figure 6: Yearly development of PV power installed [15].

PV technology has increased from less than 1 GW of installed power to near 300 GW in the 21st century with an average growth of 45% per year. This impressive growth comes from the falling prices of PV cells and modules and this trend is making the market more competitive as manufacturers have the pressure of increasing the efficiency while at the same time reducing the prices, something that is reducing the revenue margins driven many competitors out of business [16].

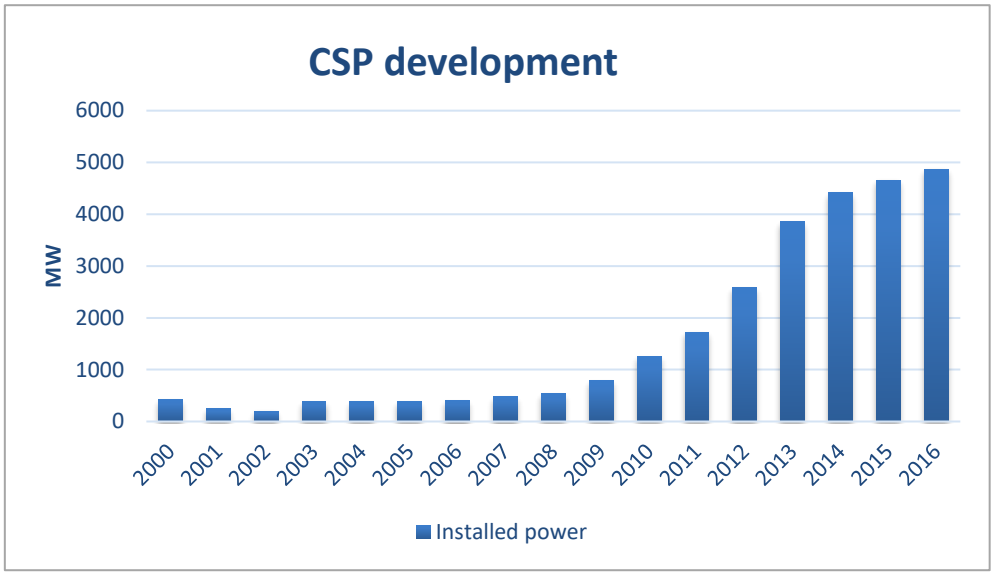

Figure 7: Yearly development of CSP power installed [15].

As shown in Figure 7, the CSP market started its real growth by 2009 driven by Spain as main contributor and finishing a period of stagnation. In the past years the growth trend has continued with increasing interest for this technology not only in power generation but also in fields such as water desalination or storage systems.

This big gap of development of one technology against the other is due to different factors, as the fact that CSP works only with direct irradiation while PV systems can also use the diffuse radiation, something which reduces the optimal areas for CSP installations. Also, CSP is only suited in large scale projects while PV can become a way of developing distributed and decentralized power. These are not the only technical factors that have increased the gap. The simplicity of PV panels and its low costs of operation and maintenance is a benefit that has helped PV deployment against the drawback for CSP of having a more complicated working system. These facts have made the market for PV panels much greater than CSP during the past years [17].

The world is moving toward a more dependent solar energy system but the situation is far from reaching its maximum potential. The IEA predicted that for the year 2050 solar power technologies will have a participation in the energy mix of 20%, while nowadays is only representing the 0,2% of the world electricity production [18], [19].

1.2.1. SOLAR INTERMITTENCY

One of the main drawbacks that solar energy presents is its intermittency, a fact that make this energy source reliable only during part of the day. This diurnal variation is also accompanied by the changes of weather conditions that can variate the output power every minute and every hour.

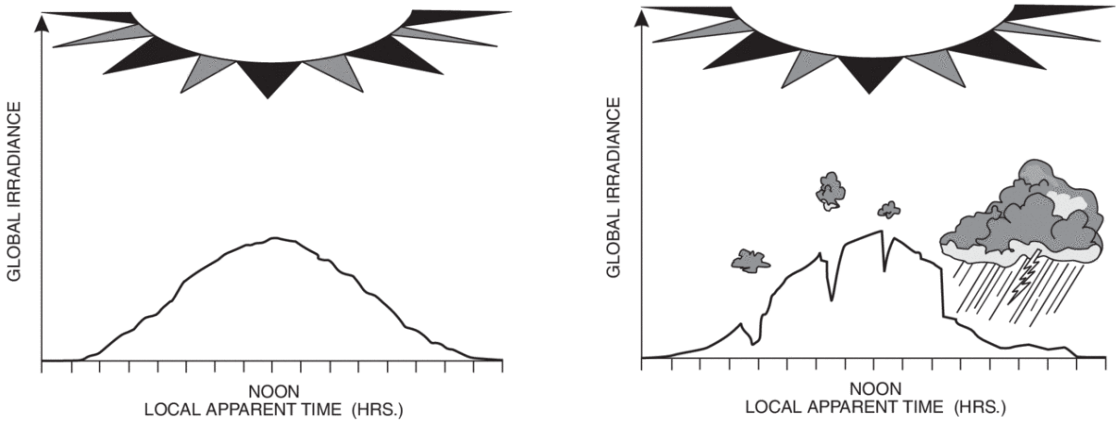

Figure 8: Intermittency of the Solar source. a) Diurnal intermittency. b) Hourly intermittency [20].

For these reasons, the solar resource must have a backup system from other type of energy source or be able to store energy for using during these intermittency periods. Both solutions have been studied already and one with the most promising perspectives is the use of heat storage of molten salts, something that could push the CSP market toward a better position. The use of batteries is also studied for PV systems but so far the costs should be reduced in order to have profitable projects as Bernhard Beck explained after presenting its pilot project of battery storage facility at large-scale PV plant [21].

For future perspectives, the storage systems are a key component for the development of renewable energies and there already exist many projects that try to reduce costs and increase the efficiency. The development of cost effective energy storage systems will allow to provide a large percentage of the world electricity from renewable sources.

The increase of efficiency that the base project looks for could mean an increment of the attractiveness of CSP plants with storage capacity and in turn this will mean more investments on a sector that tries to erase the intermittency problem.

One of the references in the tower thermal solar power sector is the Gemasolar plant located in Seville and with 19,9 MW of nominal power. This power plant counts with a thermal storage system able to generate electricity during 15 hours [22].

1.3. PV TECHNOLOGY

The functioning principle of the PV modules is based on the photoelectric effect. This effect was observed by Heinrich Hertz in 1887 and consists on the emissions of electrons from a semiconducting material under the action of radiation.

The PV cells are formed by semiconductor materials and are the ones able to convert the photons coming from the solar radiation to an electric current.

The most common material used is silicon.

The PV systems can be divided in three groups differentiated in how they interact with the grid:

- PV systems connected to the grid
- PV systems isolated
- Hybrid PV systems

1.3.1. SPANISH PV DEPLOYMENT

Photovoltaic devices use the photoelectric effect for producing directly electricity from the solar radiation.

The PV systems are the solar technology with higher development, as shown on previous graphs, and the one which is improving its efficiency every year. In an industrial scale its efficiency is set to 16% while the new world record has been stablished over 26% [23].

This technology has as main advantage the possibility of producing electricity directly from the solar radiation in an extended power range. This fact makes it perfectly fit for isolated regions where is hard to bring the electrical grid.

As we could see from Figure 6 globally solar PV industry has been growing in a continuous way and this trend is set to continue. In the case of Spain, the installed power corresponded to 4871 MW in 2016. On the following graph, it is shown how the installation of PV systems has developed during the past years.

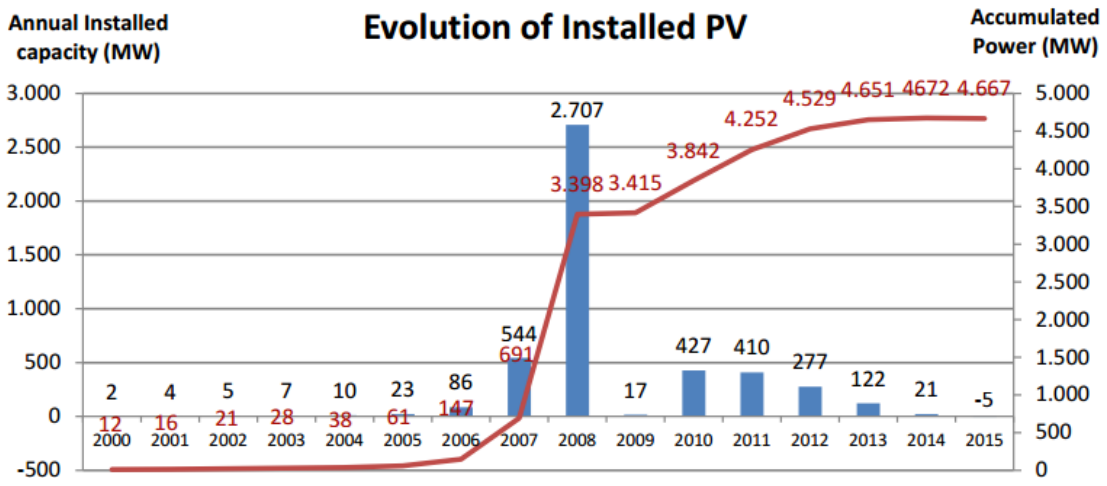

Figure 9: Evolution of PV systems installation in Spain [24].

As we can see from Figure 9 the biggest contribution to the power installed came in 2008 driven by an encouraging legislation that tried to empower the sector giving incentives and subsidizes to new installations. This legislation is summarized in the royal decrees 436/2004 and the 616/2007.

The abrupt stop of new installations after 2008 and specially after 2011 is due to the normative changes during this years. Something that created insecurity on the investors and even legal actions against the Spanish government through international arbitration.

The future perspectives in the PV market are positive even without incentives. Due to already mentioned situation in Spain, the installation of new PV plants seems that is going to continue slower but for the rest of the world the transition to solar energy sources is unstoppable.

1.4. CONCENTRATED SOLAR POWER (CSP)

Thermal power plants use the solar radiation as heat source for increasing the temperature of a thermodynamic fluid which will be used in a thermal cycle for electricity generation.

This final project is focused on thermal energy type which is less developed than photovoltaic systems as we saw on the previous graph. In 2016 there were 4.8 GW of CSP installed against the 290.8 GW of PV around the world.

CSP technology has the main advantage of being more flexible than other renewable technologies, something that improves energy security and reliability. This characteristic is due to its capacity for storing heat energy for short periods of time. This stored energy can be used when the working conditions are not optimal as cloudy days or at night. CSP plants can also have a backup technology from combustible fuels.

These factors make CSP technology able to compete with not intermittent energy sources for producing electricity when needed.

There exists also the possibility of using CSP technologies for producing concentrating solar fuels (CSF), a process under research. This could help to decarbonize transport.

CSP development is concentrated in mainly Spain and the United States accounting for more than 80% installed capacity in the world as we can see on the following diagram:

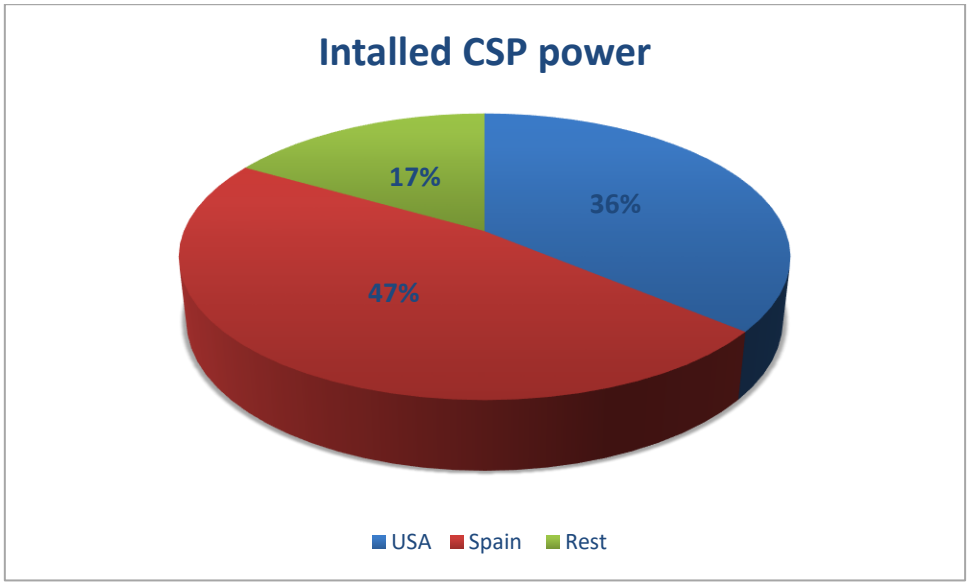

Figure 10: World CSP installed capacity [15].

This concentrated distribution is not casual. The importance given by the governments toward this technology did not really start until the petroleum crisis during the 1970 decade. At this time, the US started pilot projects looking for less dependent source of energy but without reaching the commercial level.

The following step toward a higher deployment of CSP technologies was triggered by the ambient concerns increased at the beginning of the 21st century. Helped by regulatory conditions on 2000, the thermal power technology started to reach a commercial level and different thermal power plant types were studied. Spain gave a big impulse when in 2007, driven by subsidizes and potential revenues, a great capacity started to be installed until it stopped in 2013.

1.4.1. CONCENTRATED SOLAR POWER TECHNOLOGIES

The thermal power technology installed is divided in three main types differentiated in the method used for concentrating the solar rays:

- Parabolic trough
- Parabolic dish
- Solar tower

1.4.1.1. PARABOLIC TROUGH AND FRESNEL REFLECTOR

The parabolic trough operating principle consists on reflecting the light of the sun, using a parabolic reflector, towards an absorber tube which contains the heat transfer fluid (HTF) and is located at the focus of the concentrator. This technology is also equipped with a solar tracker that follows the trajectory of the sun.

The Parabolic trough power plant type is nowadays the one with highest presence on the CSP market with around 85% of the total capacity installed [25]. This type takes its name from the shape of its reflector which is aligned on a north-south axis.

Related to this type there is the Fresnel reflector that follows the same principle but in a simplified way focusing on a smaller scale due to its lower efficiency and cheaper cost. It has several flat mirrors instead of only one as the Parabolic trough.

The parabolic trough solar power plant is the oldest technology on the CSP sector. There have been studies for different fluids as water, air, oil, or nitrate salts, being nowadays synthetic oil the HTF most used on this type of plants. The temperature of the absorber tube can increase until 400 °C [26].

a) b)

Figure 11: a) Parabolic Trough. b) Fresnel.

1.4.1.2. PARABOLIC DISH

This technology has different features than the previous explained. Each device has a single reflector, with parabolic antenna shape, and it is equipped with a small heat engine on the collector point. This allows it to reach temperatures around 1000°C enhancing the efficiency. Another important feature is the lack of need of cooling water, something that makes them specially fit for arid locations. Comparing this technology with the rest CSP devices we can say that it is the one with higher efficiency and that the main drawback of this technology is its low production, in average each device can provide 25 KW. For this reason commercial power plants have not been yet constructed but only semi-commercial projects without promising results [27]. The Maricopa project was shut down in 2011 and the company that built the second project in the Tooele Army Depot in the U.S. state of Utah, fell in bankruptcy in 2013 [28], [29].

Figure 12: Parabolic Dish at Maricopa power plant.

1.4.1.3. TOWER CSP

The radiation from the sun is reflected with the help of a field of heliostats toward the top of a tower where the receiver is located. On the receiver, the circulating heat transfer fluid is heated up and is carried toward the thermodynamic cycle where exchanges its heat energy with water producing vapor which in turn is used in a turbine with a generator attached for electricity production.

The market share of this technology type is around 10% as specified on the Global Outlook 2016 report [25].

Figure 13: Gemasolar thermal solar power plant.

1.4.2. DESCRIPTION OF A THERMAL SOLAR POWER PLANT WITH CENTRAL RECEIVER

The working principle of a tower thermal solar power plant has already been explained but for a deeper understanding we will divide its parts in 5 sections giving a brief description of each one with a higher focus on the receiver system which is the main component under study during this final project.

The plant presented on the following figure corresponds to the type that this project studies, with molten salts as heat transfer fluid. This is the most common HTF nowadays for this type of thermal solar power plant but it also can be used air or steam.

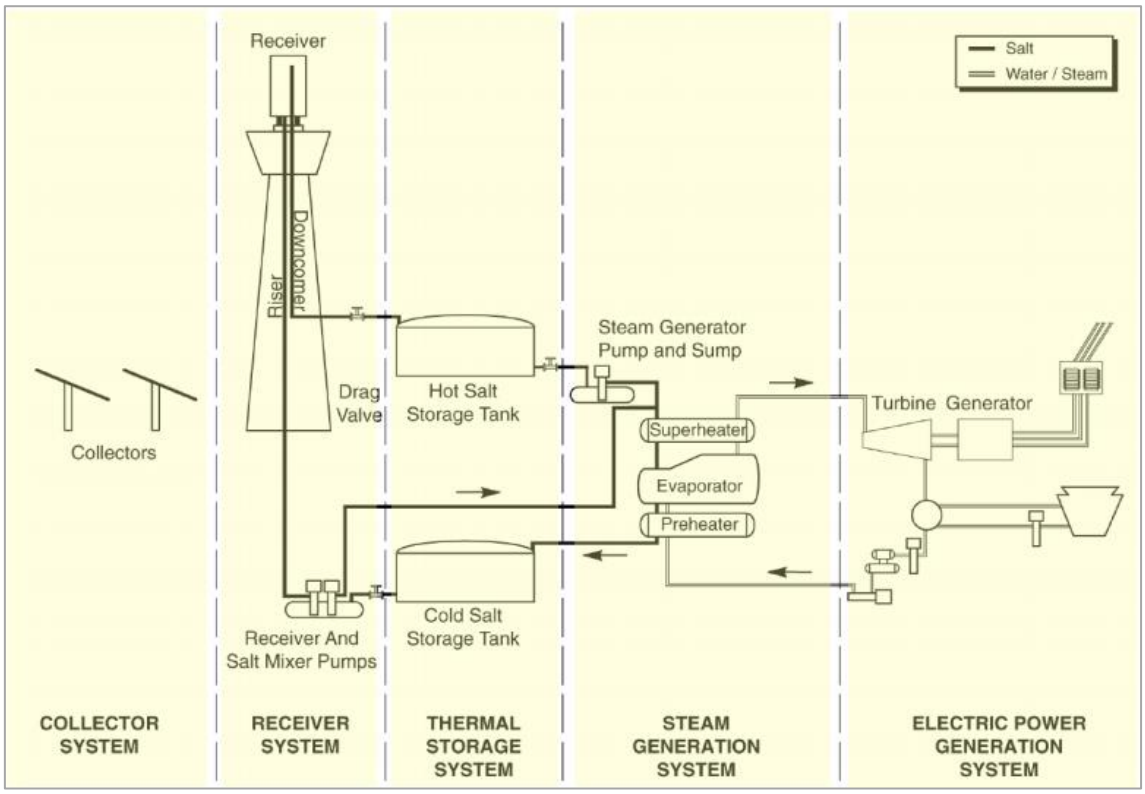

Figure 14: Sketch of a typical tower solar thermal power plant [30].

1. The collector system

It is composed of the heliostat field and corresponds to the highest investment costs of the plant. A heliostat can be considered a device containing a movable mirror which tracks the sun and reflects sunlight in a fixed direction. The overall efficiency of the plant depends in a relevant degree on the heliostats field, for this its election must be accurately performed.

2. Thermal storage system

It is composed of two tanks, one receives the hot HTF from the receiver and from the other one the salts are pumped toward the receiver. The high temperatures reached by the molten salts allow a better storage than other CSP technologies using fluids such oil. This system main advantage is that increase the capacity factor of the plant.

3. Steam generation system

It is as the ones in conventional power plants but instead of a boiler using fossil fuels the heat exchanger uses the HTF at high temperature to evaporate water and produce steam.

4. Electric power generation system

Also, it is composed of conventional devices. The steam moves the turbine which is attached to a generator that produces electricity. After passing through the turbine the vapor is introduced in a condenser which produces a phase change preparing the water for another cycle.

5. Receiver system

The receiver is the part of the plant where the HTF receives the solar radiation and absorbs it in heat form. The functioning of this part of the plant is a key feature for the overall efficiency of the plant.

This project is focused on the study of the receiver of solar tower power plants and looks for a better understanding of the enhancing measures that can be done for improving the efficiency in the transmission of the solar radiation to the molten salts circulating. This transmission produces high temperature conditions on the receiver, a fact that makes necessary to have specific materials able to withstand the stresses produced by these high temperature ranges.

As already explained the receiver is located at the top of a tower in order to be visible to all the heliostats located at ground level. This configuration makes mandatory the existence of a pump able to impulse the molten salts to the height needed.

The geometry of the receiver has been an intense field of study during the short life of the technology and for this there exist different configurations divided on receivers of cavity or external and from this last type we have to mentioned the flat, cylinders and semicylinders types [31].

The way of transmission of the solar radiation has also different configurations from direct absorption to indirect absorption, the latter covers the tubular, plate and the volumetric [31].

For the experiment studied we have simulated a cylinder with tubular configuration and with molten salts as HTF as already mentioned.

1.4.3. SPANISH LEGISLATION IN THE CSP FIELD

The development and progress of the thermoelectric power plants have conditioned the Spanish regulation of this technology in terms of retribution and growing of the thermal power plants.

At the beginning, there were incentives to new generating technologies from renewable sources which translated in a big increment of the installations in a short period of time. This fact made the whole electrical system to be insecure financially.

The first normative regarding the thermal solar power plants was presented in 2007 by the Royal Decree 661/2007. For the first time, this type of generating plants were regulated due to its previous lack of development in a commercial phase. This legislation protected the investors when the inflows were too low but it also eliminated the incentives when the benefits were too high. This Royal Decree along with previous ones put in danger the sustainability of the electrical system producing an increasing tariff deficit[1].

The Royal Decree Law 6/2009 approved the social bonus which is one of the basis for the development of the renewable energies and specially the thermal solar technology. This Decree was focused on the decrease of the tariff deficit with the objective of having by 2013 all the costs of the regulated activities covered by the taxes paid by the consumers for accessing the electrical network.

Royal Decree 1565/2010 which was formulated to guarantee the optimal operation of the technologies inside the group of special regime while sustaining the security of the electrical system. With this Decree, the thermoelectric solar power plants could increase their installed power.

The Royal Decree 1614/2010 contained changes in the regulation of the thermoelectric solar power plants regarding the selling options and incentives framework. It limited the hours of functioning with incentive tariff and imposed the selling method to be of regulated tariff during a period of time, while before the option of retribution by the so called “Mercado más prima” was contemplated.

The great development of the technologies under special regime produced an increment on the differences of the tariff deficit. This fact triggered the decision of reduction of the incentives provided to the new installations not listed on the so called “Registro de Preasignación de Retribución”. The Royal Decree Law 1/2012 implemented this reduction.

[1] Tariff deficit is the difference between the costs of generation and transportation of electricity by the companies with the actual payments of the consumer.

The next step toward a more sustainable electric system was the Law 15/2012 in which was imposed a tax of the 7% of the retribution of all the energy production plants.

The Royal Decree Law 2/2013 modified again the selling options for the installations under special regime. Its objective was to correct the tariff deficit without increasing the costs for the consumers. With this Decree, the security of the investors was eliminated and the incentive passed to be of 0 c€/KWh for all the installations under special regime.

After this summary of the past legislation the actual normative is presented.

After trying, with the previous measures, to reduce the tariff deficit without good results the Royal Decree Law 9/2013, the Law 24/2013 and the Royal Decree 413/2014 tried to unify the past normative and reduce the existent inefficiencies.

The Royal Decree Law 9/2013 imposed a new retribution regime affecting the renewable, cogeneration, and residual energy, along with new taxes. It tried to ensure the stability of the electrical system.

The Law 24/2013 eliminated the special regime in which the thermal solar power plants were contain and tried to share the debt produced by the tariff deficit between the different agents of the electrical system in proportion with their collection rights.

Finally, the Royal Decree 413/2014 stablished the legislation regulating the benefits from renewable energies during the period 2014-2019.

1.4.4. SPANISH CSP SITUATION

As we saw on Figure 10, Spain is the leading country in the utilization of thermal solar power plants with more than 40% of world installed power. Because of this, the Spanish companies are exporting their knowledge to other countries by means of participation in several projects. Nowadays there are 23 projects under construction that will be added to the 93 operational plants already functioning [32].

The leading situation of Spain will not last long with the already mentioned growth of countries investing in new installations and due to the inactivity of Spain during the last years as we can see on the following diagram:

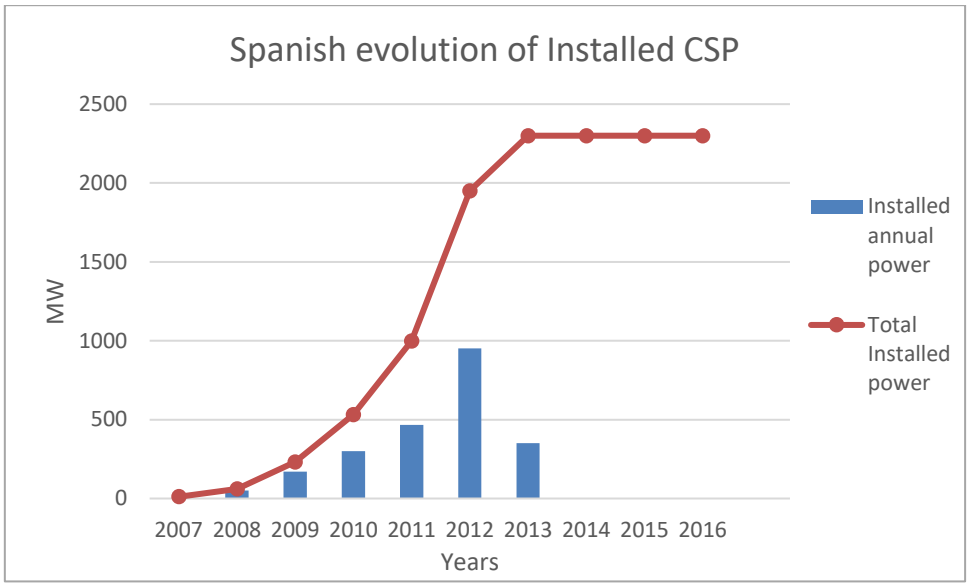

Figure 15: Annual evolution of the installed CSP power in Spain [33].

As we can see from Figure 15 the installation of new power in Spain stopped abruptly in 2013 and there are not perspectives of new investments in the near future. This fact can be better understood along with the CSP legislation section where it is already explained the cut of incentives produced from 2010. Also, this abrupt change of legislation has made several companies to apply to international arbitraries in order to receive a compensation from the Spanish government.

2. PROJECT DESCRIPTION

The experiment being held in the laboratories of the department of thermal and fluid engineering at the university Carlos III of Madrid is about the design of central receivers in thermal solar power plants. The concentrator is common to all the technologies related to electricity generation with solar thermal power and its design affects directly the efficiency of the plant and at the same time its life span and safety operation.

The increment of efficiency goes along with the increase of the working temperature but this high temperature results in the emergence of thermal tensions which are also due to the corrosivity of the working fluid. These thermal tensions could suppose plastic deformations in the worst scenarios. For this reason, the experiment that this project covers was constructed. Its objective is summarized as the study of the thermal distribution in the tubes walls for estimating the energy losses and the calculation of the thermal tensions suffered by the structure.

The project that this report is presenting will be focused on three of the main steps of the research fund by the Spanish government and which has higher objectives. First the preparation and start of the installation, second the realization of experimental measurements and finally the numeric simulations and validation of the experimental results.

This final project shows two sets of experiments. The first consisting in the circulation of the molten salts through the installation, and the second consisting in the use of the inductor machine for study the increase of temperature of a tube filled with water. The final experiment will combine both experiments and will make use of the inductor machine for increasing the temperature of the circulating molten salts. Due to problems related with the inductor machine manufacturers this mentioned final experiment will not be covered in this report.

2.1. INSTALLATION AND COMMISSIONING OF THE EXPERIMENT

When I started my contribution to this experiment the whole structure was already built so we started preparing the details for the acquisition of the data. Before going deeper on the specific work on the commissioning of the experiments, a brief introduction of the installation is needed.

2.1.1. INSTALLATION

The installation under study is prepared to simulate the functioning of the receiver of a tower from a concentration solar power plant. In order to simplify the description process, the whole system will be divided in two main parts which correspond to the two experiments performed during the study. Before explaining the installation of both experiments the common features should be explained.

2.1.1.1. COMMON FEATURES

1. Thermocouples

A common feature of both experiments are the thermocouples that measure the temperature at different points of the experiments, the chosen thermocouples are of type k with a diameter of 1,5 mm and a standard accuracy around ±2.2 °C [34]. These devices are the most common type of thermocouples and can be considered as simple, cost-effective, and robust temperature sensors. They are composed of two different metal wires joined at both ends. When one end is heated the Seebeck effect is produced, this effect consists on a continuous current flow in the circuit formed. If this circuit is broken at the middle the open circuit voltage is a function of the temperatures and the wires composition. This means that this voltage measured can be correlated to the temperature applied [35].

The thermocouples will be located at critical points of the installation where a temperature control must be applied and also at points of interest for the heat transmission study. On the experiment section, the location of the thermocouples is shown in more detail. These devices are a key tool for the study but in some of the experiments we could not count with all the installed thermocouples due to their damage during operation.

2. Data acquisition card

Another common feature of both experiments is the data acquisition cards. These devices are fundamental for the results because they are the ones that receive the information from the thermocouples and pass it to the computer for further study. The acquisition cards used during the experiments are a OMB-DAQBOARD-3000 Series which are characterized by their high speed, low latency, and highly deterministic control output mode [36].

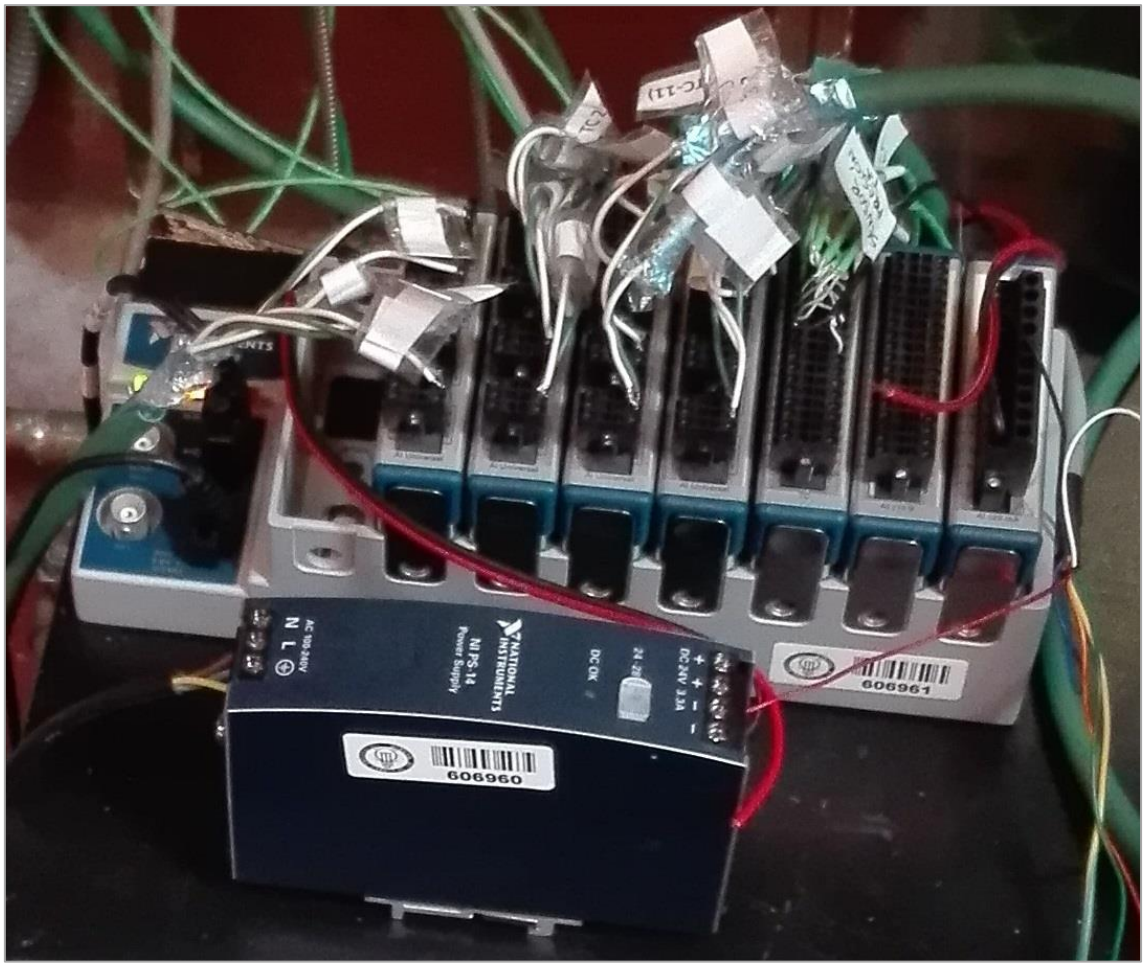

Figure 16: Acquisition data device.

From the previous figure, we can distinguish several acquisition cards with different input connections. The use of the cards is divided in the ones that received information about the temperatures, the one that receives the pressure measurements and finally the one that translates the measurements of the voltage. Once connected to the computer, each input must be identified by a code in the software LabView in order to label the results obtained.

2.1.1.2. CIRCULATION EXPERIMENT INSTALLATION

For the experimental part concerning the circulation of the molten salts we will describe the HTF transport subsystem:

This subsystem is composed of the needed elements for the transportation of the molten salts on a close cycle which simulates the tubes of a real receiver. In an operative CSP plant, inside the tubes of the receiver the molten salts increment their temperature due to the radiation concentrated by the heliostats and continue their path towards a hot storage tank or directly to a heat exchanger. For our case study, the molten salts will return to a tank from where they will be recirculated as many times as the experiments require.

This subsystem can be divided in three main parts:

1. Tank
2. Pump
3. Tubes

Figure 17: Circulation of the molten salts experiment installation.

On Figure 17 we can appreciate a picture of the components that englobed the subsystem previously mentioned. The components that we can see pointed are the tank, the pump and the loop formed by the tubes respectively.

For a better understanding we will revise each main part:

1. Tank

The tank is composed of stainless steel 316 with properties and dimensions summarized on Annex 1.2. On the following image, the visible part of the tank is shown.

Figure 18: Storage Tank where the molten salts are melted.

On the tank, the salts are concentrated and melted with the help of two resistances located one on the interior wall and the other one on the bottom. For reducing the heat losses, the tank is covered by an insulation material called rockwool with a thermal conductivity variable with the temperature following the formula:

$$K_{\text{rockwool}} = 0{,}0002 * T(^{\text{o}}C) + 0{,}0252$$

From the tank, the salts will start their transportation cycle from the deposit which is inside of the tank and where around 600 liters of salts are stored. This part must be completely isolated because a leak of the molten salts during their circulation could be dangerous due to the high working temperatures of the fluid.

Another important part of the tank consists on the thermal heaters located inside. These resistances are the main component of the temperature control system of the tank. They are controlled for increasing the temperature of the salts until the working temperature is reached and not surpassed the limits imposed, for this objective two resistances have been installed. One is a panel heater under the tank and the others are semi cylinders heaters located on the walls of the tank. The properties and dimensions of the two resistances are attached on Annex 1.3 and 1.4.

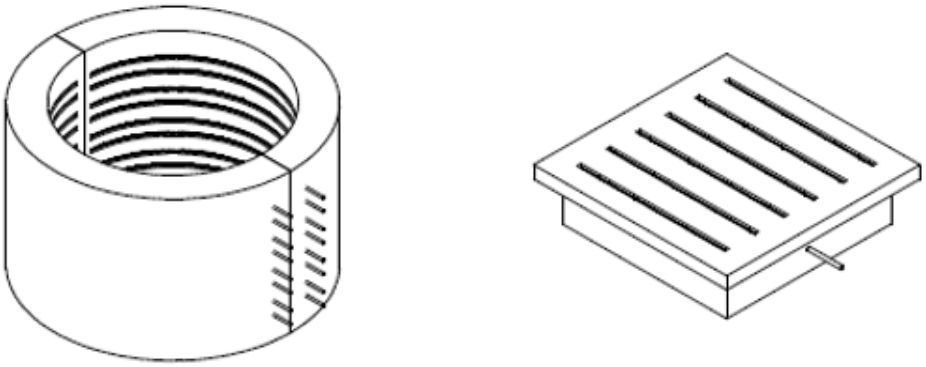

a) *b)*

Figure 19 : a) Resistance at the wall of the tank. b) Resistance on the lower part of the tank.

2. Pump

It is the main component for the circulation process. Its function covers the pumping of the fluid from the tank to the tubes at enough power to circulate the HTF through the loop. It is an industrial pump and its rotational frequency can be regulated. This possibility of regulation allows us to study the experiment at different conditions of mass flow, something that shows the best suited velocity of the molten salts for reducing the heat losses and the thermal stresses inside the tubes. The properties of the pump are attached in Annex 1.5. The observable part of the tank is shown on the following image:

Figure 20: Visible section of the pump.

As we can observe from Figure 20 the shaft of the pump is painted in white in order to see if the pump is working from the outside of the room when the circulation process has started.

3. Tubes

Are the ones that take the molten salts from the tank to the simulated receiver and back to the tank conforming the circulation cycle. The tubes are also covered with the same isolating material used around the tank except for two important sections. The first section is located at the upper tube, where the simulation of the solar radiation with an inductor will take place. The second non-isolated section corresponds to the lower tube which returns the molten salts to the tank and where a flowmeter is located. The reasons for not isolating this later part are due to the specifications of the manufacturers for ensuring the good functioning of the flowmeter. On the technical datasheet is explained that with isolating material the transducer equipped inside the flowmeter will surpass the ambient temperature being this limit the maximum temperature allowed [38].

Another tool of the circulation cycle consists on a bypass valve that regulates the amount of salts pumped near the tank outlet.

Figure 21: Circulation loop with the non-isolated sections pointed.

From the picture, it is appreciable the inclination that the structure has. At the beginning of the dimensioning of the experiment it was decided that an inclination of this type could help the return of the salts to the tank once the circulation process stopped. This is essential for avoiding the solidification of the salts inside of the tubes, for this purpose also an electrical heat tracing is installed through the tube as explained in the following pages. In real plants the solidification of the molten salts is one of the main concerns due to the problems associated that have a final repercussion on the maintenance and operation costs [39].

The molten salts are pumped from the tank and start the circulation through the upper tube passing through the inductor section and returning from the lower tube passing

through the flowmeter which measures the velocity of the salts passing. With this value and the variable density of the salts we can calculate the mass flow following the formula:

$$\dot{m}salts = V * Ain * \rho salts$$

With:

$$V = Velocity\ measured\ by\ the\ flowmeter$$

$$Ain = \pi * \frac{Dint^2}{4} = Area\ inside\ the\ tube$$

$$\rho salts = density\ of\ the\ salts\ for\ a\ given\ temperature$$

3.3 Electrical heat tracing

The objective of the electrical heat tracing is to maintain the temperature of the tubes, flanges, and valves of the circuit at the specified set point. This set point can be selected on the control panel of the installation and normally will be 300 °C. The electrical heat tracing is divided in two sections, one longer than the other, that cover the total tube installation but for the section where the inductor will be located. The importance of this system is to avoid the risk of solidification of the salts inside the tubes, an inconvenient that could cause additional costs and losses of time as already mentioned.

The cable is encapsulated by a dielectric of magnesium oxide and covered by a metallic layer. The heat is generated in the conductor by the Ohm law and the Joule effect [40].

The design parameters of the cable are summarized in the Annex 1.7.

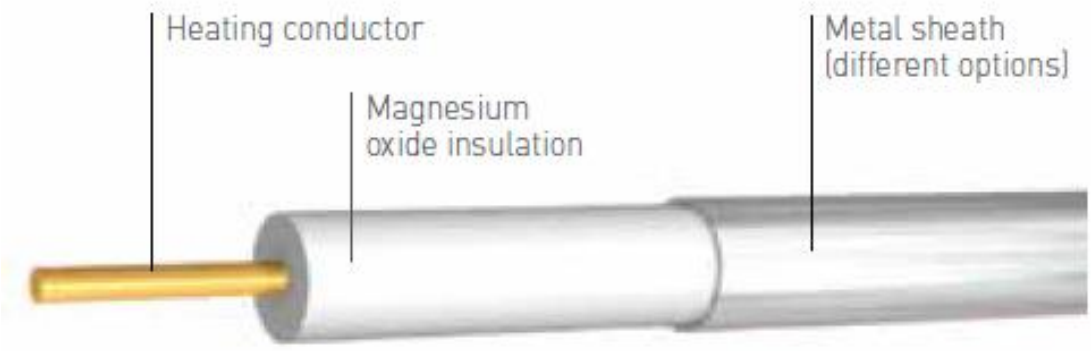

Figure 22: Electrical Heat Tracing diagram.

2.1.1.3. INDUCTOR EXPERIMENT INSTALLATION

For the experiment related to the warming of water inside a tube we will describe the structure with special attention to the inductor machine. A key component for future goals of the university concerning the simulation of solar radiation.

Figure 23: Inductor experiment installation.

On Figure 23 we can see the experiment installed. The main components used are:

1. Inductor machine:

As explained before this component will be the one able to simulate the solar radiation concentrated in the receiver of a thermal power plant. For this, the induction machine produces a circulation of alternating current through the machine coil in order to generate a magnetic field. The force of this magnetic field will depend on the current passing through it and on the number of turns of the coil [41]. By resistive heating the temperature of the metal tube increases and with it the water deposited inside. The main benefits of using this type of technology are the high heating ranges obtained, the

contactless energy delivered, the safety operation, and that the heating process occurs rapidly.

An ac source provides the alternating voltage to the inductor coil generating a magnetic field in which the tube is immersed. The heating process is mainly due to the Eddy currents which produce the heating by Joule effect [42].

This type of machine is able to operate at different modes by creating heat sequences which allow to variate the power input and the time applied.

The induction system is a Sinac 6 SH 350 KHz with TSC Heating Station. This type of machine can be divided in three main subsystems:

- Frequency converter and Control Panel
- Magnetic flux concentrator
- Induction coil

1.1 Frequency converter and Control Panel

Consist on the main part for adjusting the require needs. It is located inside a cabinet, which protects it, along with indicators and switches. For the interaction with the operator there is a screen and a keyboard that allows to change the parameters for the working process of the machine.

1.2 Magnetic flux concentrator

Is the component that allows to focus the magnetic flux in a specific location. Without it the magnetic flux could be propagated and produce problems inside the machine.

1.3 Induction coil

Is one of the most important components of the inductor machine due to its principal role of generating the magnetic field in front of it, in our case in the surface of the tube. For its correct functioning, it is important to have a cooling system providing enough water to control the temperature of the coil. An excess of temperature could produce the breakdown of the induction coil.

The minimum requirements for the water supply are specified by the manufacturer and correspond to 10l/min [43]. Also, the water must fulfill other requirements which are summarized in Annex 1.6.

Figure 24: Inductor machine.

2. Tube

This experiment was performed following the conditions that the target experiment will have. For this the tube used has the same characteristics as the one installed in the upper part of the loop where the molten salts will be circulated. Also, axial sections of the tube will be studied by means of the measurements obtained by the thermocouples. The specific location of these thermocouples is described in the experimental procedure part.

3. Cooling system

The cooling system used during the experiments regarding the use of the inductor machine is formed by a refrigeration tank, a pump and a Daikin machine of type EWAQ005 with a nominal capacity for cooling of 5.2 kW and a nominal water flow of 14,3 l/min [44]. This machine main goal is to cool the water coming from the induction coil. The water output must fulfill the requirements previously stated in terms of quality and temperature.

The refrigeration tank main purpose is to storage the cool water in order to ensure the continuous functioning of the inductor.

The pump provides the flow needed for the optimal operation of the inductor. This machine is a Wilo MHIL 107 EM.

2.1.2. PROPERTIES

The heat transfer fluid that we will use is nitrate salt, which is a mixture of 60% by weight sodium nitrate (NaNO3) and 40% by weight potassium nitrate (KNO3), its working temperature ranges from 260°C to approximately 621°C and special attention must be paid during the experiments in order to not reach the solidification temperature inside the tubes which is around 221°C, as stated by Zavoico's report [45].

The properties of the working fluid are summarized in Annex 1.1 at the end of the report.

2.1.3. COMMISSIONING AND CORRECTIONS OF THE EXPERIMENTS

1. Salts introduction to the tank

During the first days, our work on the installation was focused on the introduction of the nitrate salt mixture inside the tank. For this process, basic knowledge of the properties of the heat transfer fluid that we wanted to achieve must be taken into account.

As explained in the properties section, our heat transfer fluid is formed by 60% NaNO3 and 40% KNO3. For achieving this mixture, we weighted different buckets of this separately salts with a weighting scale with 20 grams error and afterwards the two types of salts were introduced in a bigger container in order to remove the conglomeration and also have the two types partially mixed. We owe to remark the term partially mix because the real mixture will be achieved after the change of phase from solid to liquid inside the tank at a temperature around 260 °C as explained in the properties section.

After the partial mix process, we finally introduced them in the hot tank with the help of a ramp installed for this purpose.

The introduction of the molten salts inside the hot tank was developed with special suits and face masks for preventing us from breathing or touching the reaction compounds that could come up from the hot mixture.

The warming of the salts until phase change will be study in the following sections.

2. Adjustment of the electrical heat tracing to the exterior wall of the tube

The trace cable is an important parameter of the installation, it reduces the risk of solidification of the salts inside of the tube. This fact in a real plant is key for reducing the costs of maintenance due to the big inconvenient that this problem produces in terms of replacing of tubes and stop of the normal operation as already mentioned.

During one of the preparation steps of the installation we noticed that the trace cable which was supposed to provide at that time a temperature of 150 °C to the tube, was not affecting the temperature of the thermocouples located at the walls of the tube where the inductor would be located. These thermocouples were measuring a temperature of 60 °C. After discussing the possibilities of this high difference and observed the installation, we reached the conclusion that a metal net was needed in order to distribute better the heat provided by the cable to the tube and also that the cable should be closer adjust to the tube.

Flanges were used to put closer the cable to the tube and the metal net was installed in all the perimeter of the tube.

3. INDUCTOR EXPERIMENT. HEAT TRANSFER IN THE TUBE WITH WATER.

The inductor is the key component for achieving the goals of the experiment. As explained before it will recreate the solar radiation incident in a tube of a central solar receiver. For understanding better its functioning we prepared an experiment searching for an estimation of the heat losses produced when applying the inductor magnetic field to the exterior wall of a tube filled with water.

As explained in the inductor experiment installation section, this experiment will use the inductor machine along with the cooling system.

The needed steps for initializing the experiment in a safety manner are the following:

1. The general switch from the control panel must be positioned at its maximum right location.
2. The next step is to action the inductor.
   - 2.1 Switch on the induction machine from the control panel.
   - 2.2 From the control box of the Induction machine located inside of the experiment room the lever must be positioned at the ON position.
3. Then the refrigeration system must be switch on.
   - 3.1 From the control panel, the switch located at the left of the one marked as A/A must be rise. This switch is the one that actions the energy supply to the refrigeration system.
   - 3.2 Again, from the control panel, the switch with the label A/A must be rise. This switch corresponds to connection of the refrigeration machine.
4. For the following step, the security switch of the pump and the refrigeration machine must be actioned. This switch is located at the wall next to both machines.
5. This step consists on start the refrigeration machine by pressing the start button.
6. Finally, the pump can be actioned by rising the switch with a label reading “bomba” (pump in Spanish). This switch is next to the one with an A/A label.
7. Once these steps are completed the induction machine can be operated.

3.1. EXPERIMENT DESCRIPTION

Searching for an estimation of the heat losses during the process of heat transfer to the stainless-steel tube with the inductor as the heat source we have filled a tube with water and we have measured how the temperature was distributed throughout the tube when the inductor heated its exterior wall. For this we have analyzed different distances of the inductor to the tube and at different loads looking for a similar pattern. The experiment was conducted with a 1,5 meters long tube and with a height of water inside of the tube of 1 meter. The maximum temperatures allowed for the water were less than 100 °C in order to avoid evaporation. The tube was positioned vertically and it was surrounded by a rockwool layer for avoiding heat losses to the ambient as we can appreciate from Figure 23 in the installation section. This vertical position is the common one used in commercial solar thermal power plants.

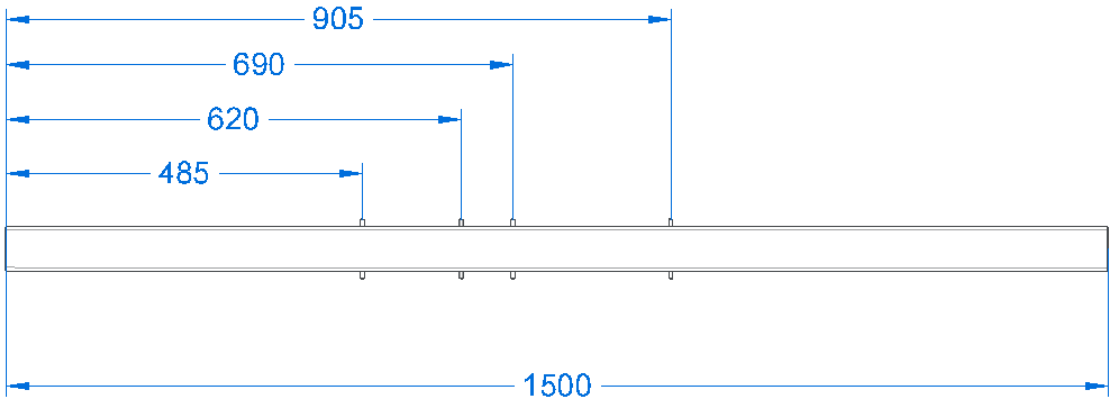

Figure 25: Dimension of the tube and location of the thermocouples.

On Figure 25 we can appreciate the most relevant distances. The tube measures 1.5 meters while the height of water will be of 1 meter as already mentioned while the other 4 measurements pointed on the figure are meant to correspond to the location of the different sections of the thermocouples with section 1 at 485 mm from the bottom, section 2 at 620 mm, section 3 at 690 mm and finally section 4 at 905 mm. These distances are not selected casually but they are closely related to the disposition of the thermocouples located at the section where the inductor will be positioned in future experiments in the circulation loop. These positions are shown in the next experiment.

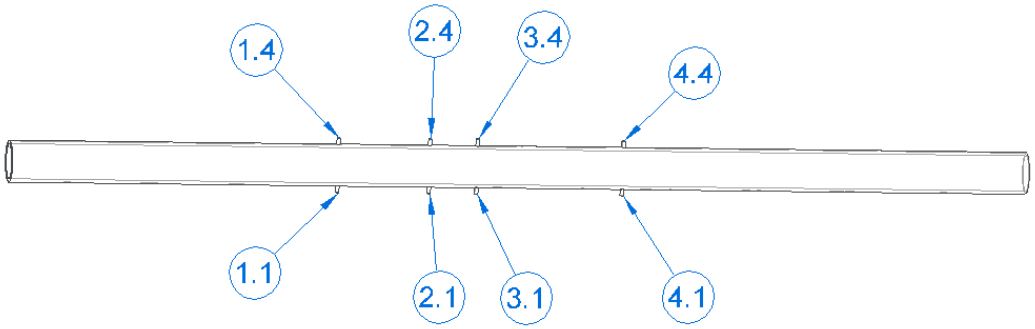

Figure 26: Thermocouples location.

The thermocouples located at the exterior wall of the tube are shown on Figure 26. There is a total of 8 thermocouples in the exterior wall of the tube and must be also remark that at section 1 and 4 two thermocouples are installed for measuring the temperature of the water inside of the tube. The other two thermocouples installed for this experiment are located at the inlet and outlet position of the cooling cycle, which pass through the inductor.

3.2. EXPERIMENTS PERFORMED

Once all the system was commissioned we have performed different experiments changing the inductor load looking for a tangible relation between the heat transfer:

Experiment	Inductor Power (W)	Time Inductor on (s)	Distance (mm)	Position of the Inductor
1	1000	2250	3	1
2	2000	724	3	1
3	3000	409	3	1

Table 1: Inductor experiments at different loads.

And changing the distance from the coil to the tube:

Experiment	Inductor Power (W)	Time (s)	Distance (mm)	Position of the Inductor
4	2000	853	3	1
5	2000	1220	6	1

Table 2: Inductor experiments at different distances from the tube.

For both sets of experiments we will refer to the functioning of the inductor already explained in the installation section and the same formulas will be applied for both studies. The position of the inductor refers to section 1 at 485 mm distance from the bottom. This data is relevant because other experiments that are not reported on this work have been performed at different heights of the tube.

3.3. FORMULAS USED DURING THE STUDY

After obtaining the measures from the thermocouples in both sets of experiment the heat losses had been calculated following the formulas:

1. Heat absorbed by the refrigeration cycle passing through the coil of the inductor. Calculated using the data measured by one thermocouple at the inlet and other at the outlet of the refrigeration loop along with the mass flow of the cooling water and its heat capacity. The mass flow of the water is calculated knowing the density of water and the volume flow, which is specified by the cooling device (82 dl/min).
2. Heat absorbed by the water, which is measured with the help of two thermocouples inside the tube at different heights. These thermocouples provide the temperature change inside of the tube along with the period of time and by using the mass of water introduced and the heat capacity we can approximate the heat absorbed by the water multiplying the mentioned factors.
3. Heat absorbed by the tube. Using the data recorded with the help of the thermocouples situated at different heights of the wall of the tube we can approximate as before the heat absorbed. This time the mass of the tube will be used along with its heat capacity and everything multiplied by the derivative of the temperature with respect to time.
4. Heat lost to the ambient and others. Calculated knowing the heat input and with the previous heat losses obtained. This heat lost accounts for all the losses that we cannot accurately measured.

1. Heat lost from refrigeration:

$$\dot{Q}ref = \dot{m}ref * Cpwater * (Tref.outlet - Tref.inlet)$$

2. Heat absorbed by the water:

$$\dot{Q}abswater = mwater * Cpwater * (\frac{dTwaterinside}{dt})$$

3. Heat absorbed by the tube wall:

$$\dot{Q}abswall = mwall * Cpwall * \left(\frac{dTwall}{dt}\right)$$

4. Heat lost to the ambient and rest:

$$\dot{Q}lost = \dot{Q}in - \dot{Q}ref - \dot{Q}abswater - \dot{Q}abswall$$

Each formula is further explained in Annex 3.

3.4. SET 1 OF EXPERIMENTS. CHANGE OF INDUCTOR LOAD.

For the set of experiments with an equal separation of 3 mm from the inductor to the wall of the tube, the inductor has been programed in three different modes for the study of the relation of the load with the percentage of heat losses.

For the data obtained only one of the experiments measurements will be shown due to the similar patterns of the other experiments. At the end of this study a comparison of the heat losses obtained from the different loads will be displayed.

The following figures correspond to experiment 1 which has as main characteristic 1KW load provided by the inductor:

1.

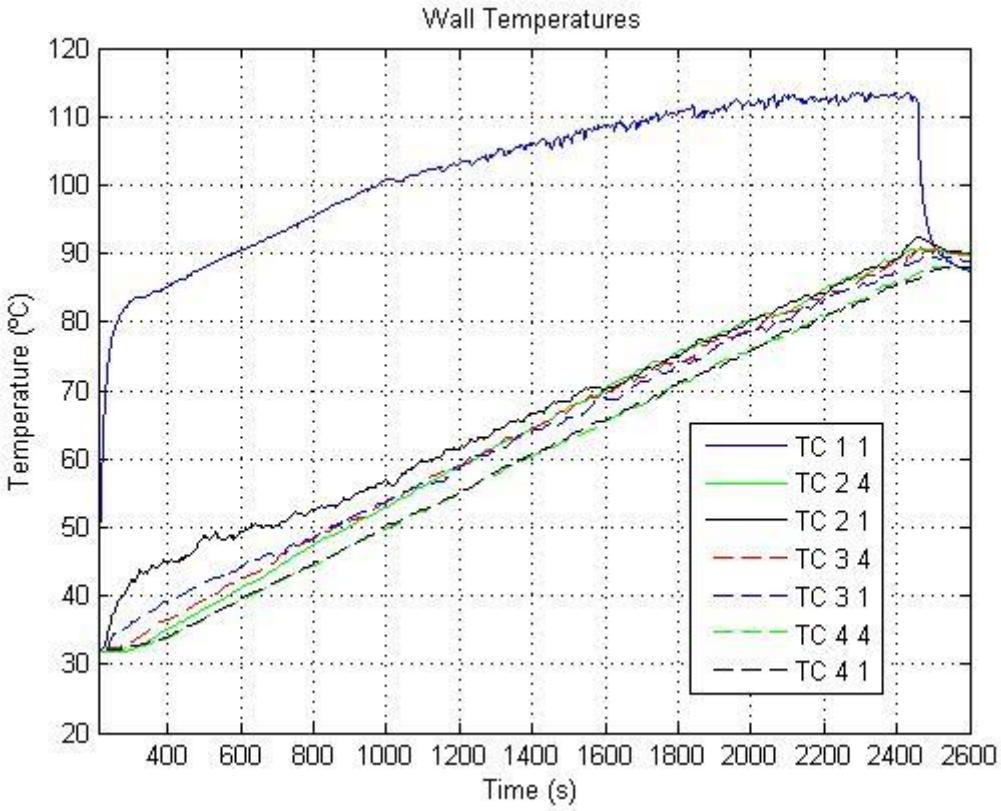

Figure 27: Inductor experiment 1. Wall temperatures.

On this graph, we can see that all the thermocouples of the wall increase their temperature measurements in a similar manner but for the temperature of the thermocouple located at the height of the inductor (TC 1.1).

With a closer look, we can distinguish better the similarity between the temperatures measured:

1.1

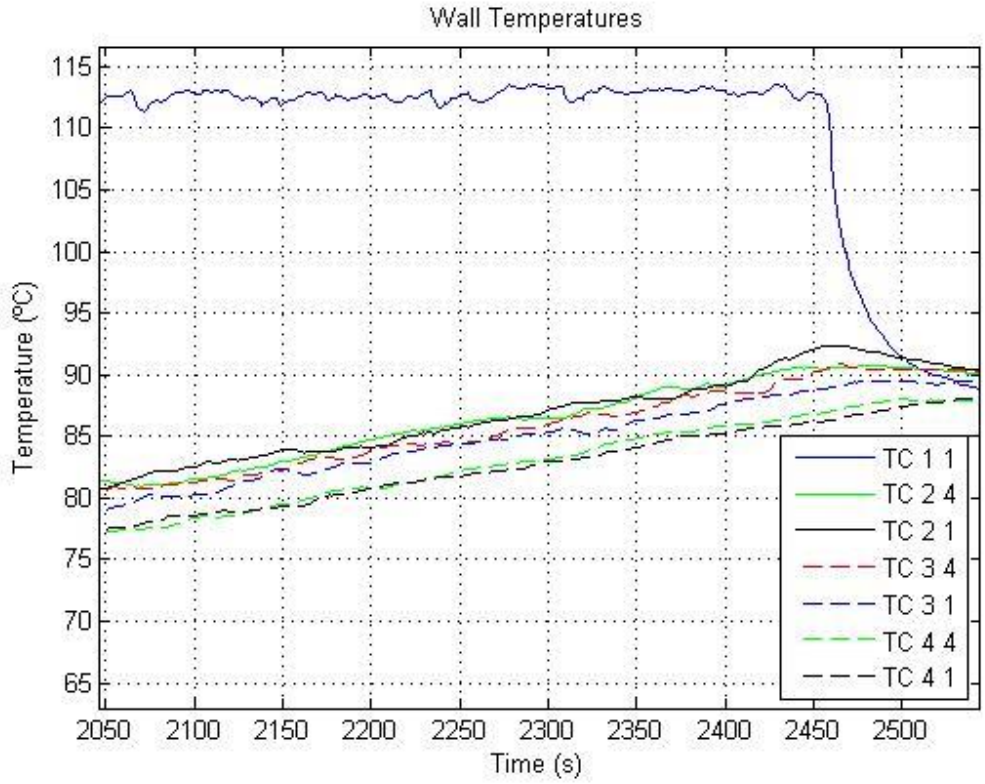

Figure 28: Inductor experiment 1. Focus at Wall temperatures.

We can observe that the differences between the lowest and the highest temperature values is less than 5°C without accounting for TC 1.1. Also, we can clearly see that the distance from the heat source affects directly the measurements being the two leading temperatures the ones located at the wall of section 2, followed by the ones measuring at section 3 and finally the ones at section 4. It is also interesting to notice that even though the inductor was applying its magnetic field at point 1.1 the measurements between points 1 and 4 are similar for all the sections, something which gives us an idea of the good distribution of the heat provided in the axial coordinates.

For the temperature of the water inside the tube we have:

2.

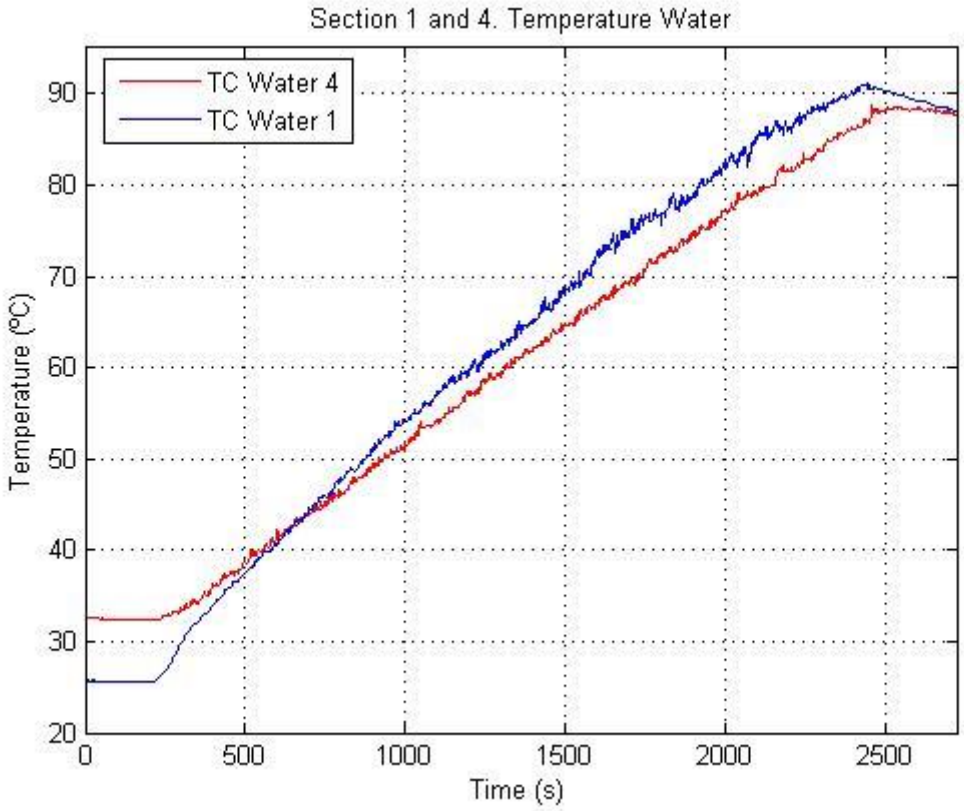

Figure 29: Inductor Experiment 1. Water temperature.

As we can see the water at point 1 increases its temperature faster due to the proximity of the inductor.

3.

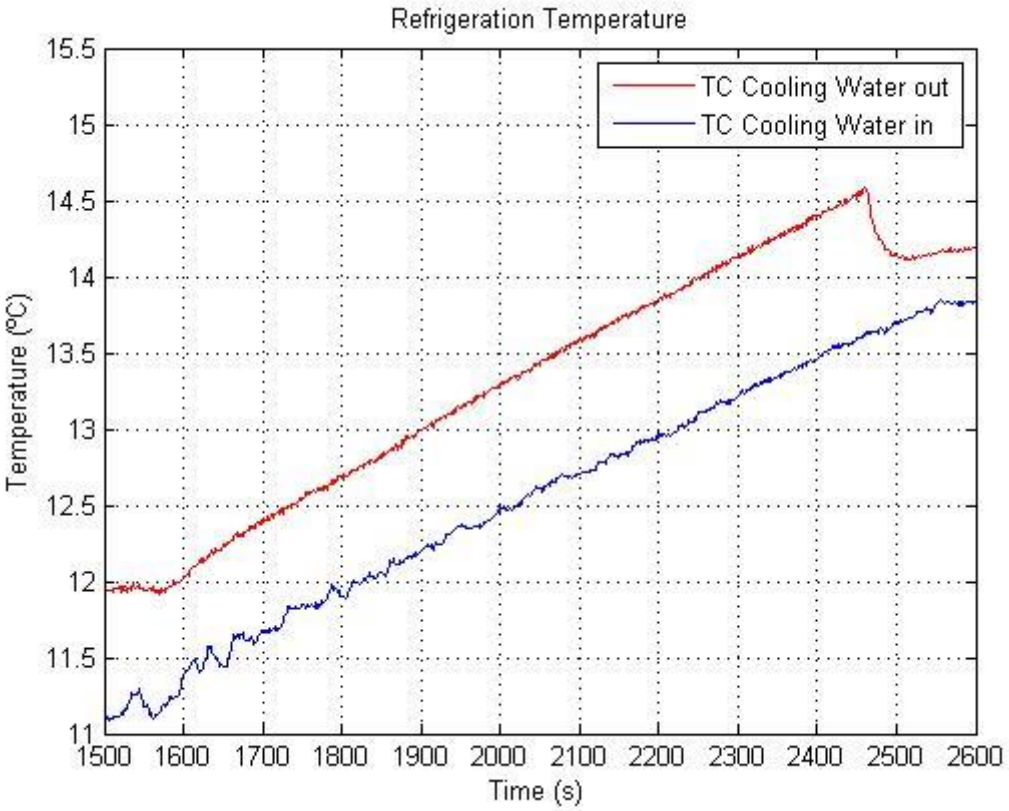

Figure 30: Inductor experiment 1. Temperature of the refrigeration water.

For the refrigeration water that goes from the cooling device to the inductor we can clearly see the increment on temperature from the inlet thermocouple to the outlet with a constant difference of around 0,75°C. This temperature change could be considered low if we do not consider the volumetric flow passing through the inductor which is high.

With this data, we are now able to estimate the losses from each shown temperature distribution and calculate the overall percentage using the formulas previously mentioned.

3.4.1. RESULTS SET 1

We have obtained the following results from the study of the heat losses:

Experiment	$\dot{Q}in$ (W)	$\dot{Q}abswater$ (W)	$\dot{Q}abswall$ (W)	$\dot{Q}ref$ (W)	$\dot{Q}lost$ (W)
1	1000	124	71	460	345,1
2	2000	449	272	977	698
3	3000	672,7	376	1503	448,3

Table 3: Inductor experiments results for different loads.

For a better understanding:

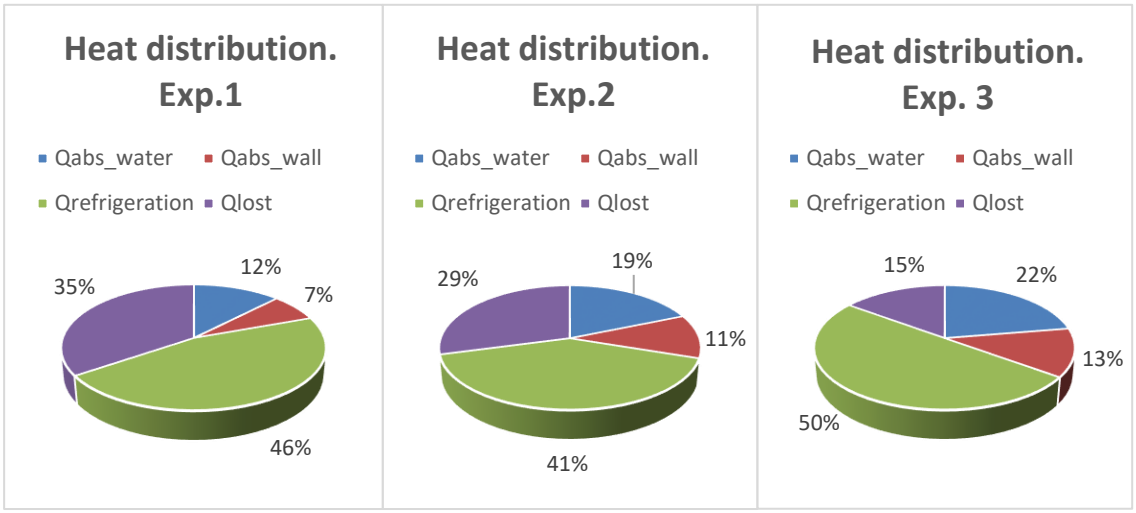

a) *b)* *c)*

Figure 31: Comparison of the result obtained for heat distribution. a) Exp.1. b) Exp.2. c) Exp.3.

From these graphs, we can clearly see the heat distribution in percentage of the different experiments, considering that the 100% will be the heat provided by the inductor in each experiment.

The conclusions reached after this study are that the percentage of heat absorbed by the water increases with the heat provided while the losses are reduced gradually. One negative feature of the results is the high percentage of heat absorbed by the refrigeration system which variates without a clear relation through the experiments but has the highest value as common characteristic of the three studies.

It would be interesting to try higher ranges of power for the inductor in following experiments in order to have more data about the heat transferred considering that the maximum power that the inductor can provide is 10 KW and on this report, we could only perform experiments with loads at 3 KW due to the damage of the flux concentrator of the inductor.

3.5. SET 2 OF EXPERIMENTS. CHANGING THE INDUCTOR DISTANCE.

As already mentioned there have been performed several experiments but only one at a distance of 6 mm from the inductor coil to the tube in order to see the differences produced in the heat transfer process. This mentioned experiment will be compared to one at the same inductor load but at a distance of 3 mm which is the one recommended by the manufacturer. For a better study, the same time range will be considered being this time the one corresponding to the heating process of the experiment at a distance of 3mm.

Also for a more accurate understanding of the results obtained, the following graphs compare the different measurements of the thermocouples. These locations can be divided mainly in three parts: Thermocouples located at the exterior wall of the tube, thermocouples measuring the inside of the tube and finally the thermocouples measuring the temperature at the inlet and outlet of the refrigeration cycle.

1. Exterior wall measurements

These measurements are divided in four sections pointed on Figure 26 as section 1, 2, 3 and 4, with two thermocouples per section except for section 1, where only the measurements of the thermocouple 1.1 were available at the time of the experiment.

1.1

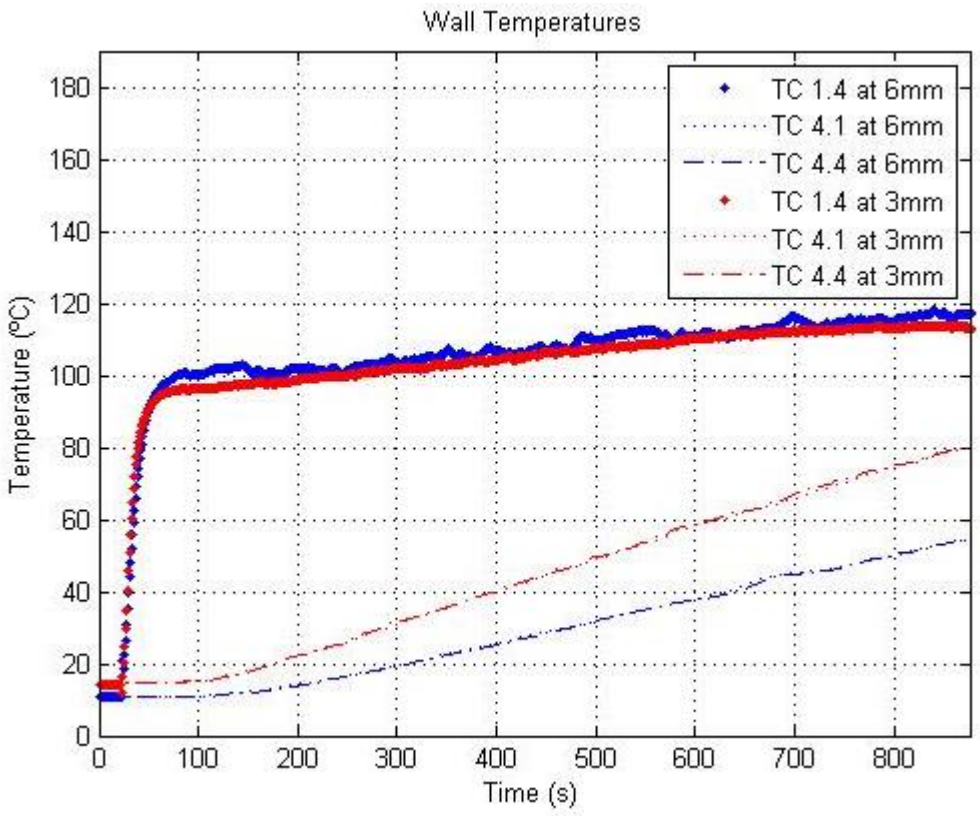

Figure 32: Experiments 4 and 5. Measurements of thermocouples at section 1 and 4 of the wall.

As we can see from the graph above the temperatures patterns are similar but with a slightly higher value for the temperatures reached by the 6 mm experiment at thermocouple 1.4, while reaching higher differences between the temperatures at section 4 where the experiment at 3 mm distance recorded values much higher than the ones for the 6 mm.

1.2

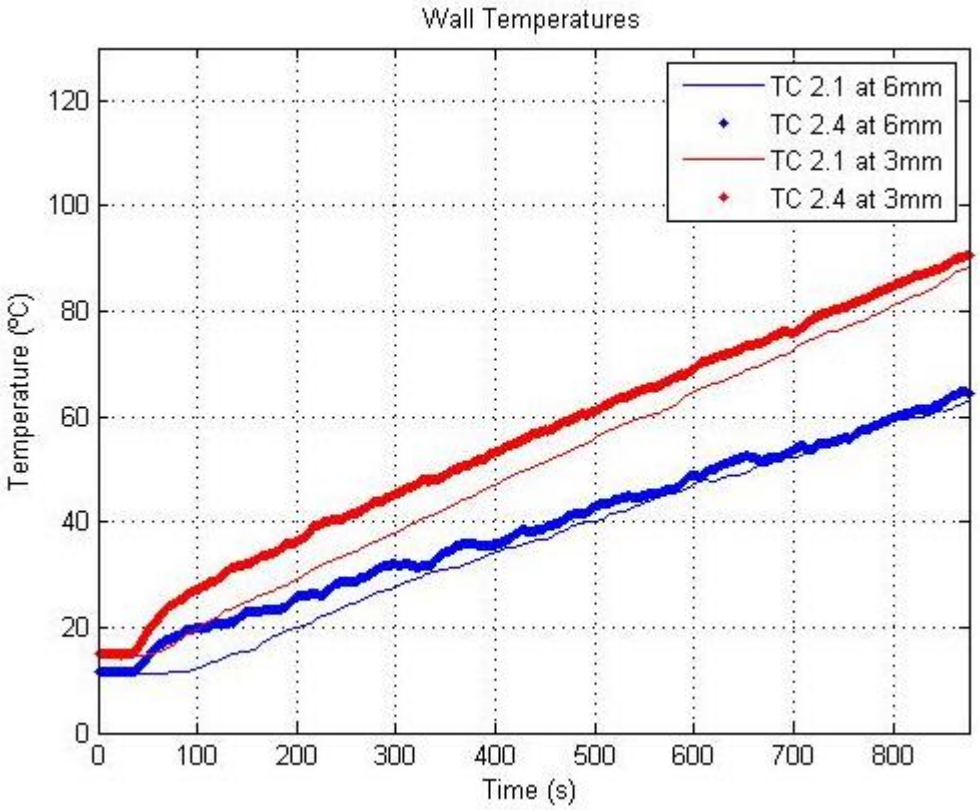

Figure 33: Experiments 4 and 5. Measurements of thermocouples at section 2 of the wall.

At section 2 we can clearly see that the temperature of the 3 mm experiments reached higher values than the one at 6 mm with, as before, a similar increasing pattern but with a higher slope in the 3 mm experiment, something which was to be expected having both experiments the same load but different distances.

1.3

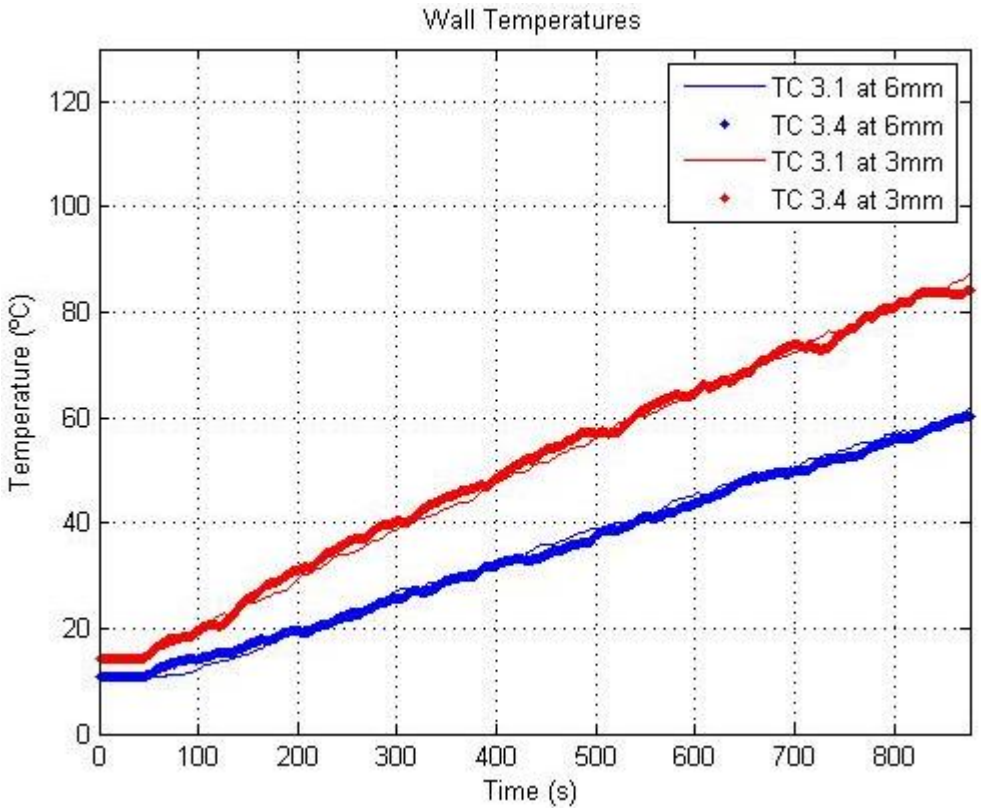

Figure 34: Experiments 4 and 5. Measurements of thermocouples at section 3 of the wall.

From this figure, we can appreciate the same pattern shown in section 2.

2. Measurements of the water inside the tube.

For the location at the inside of the tube there are only thermocouples located at section 1 and 4.

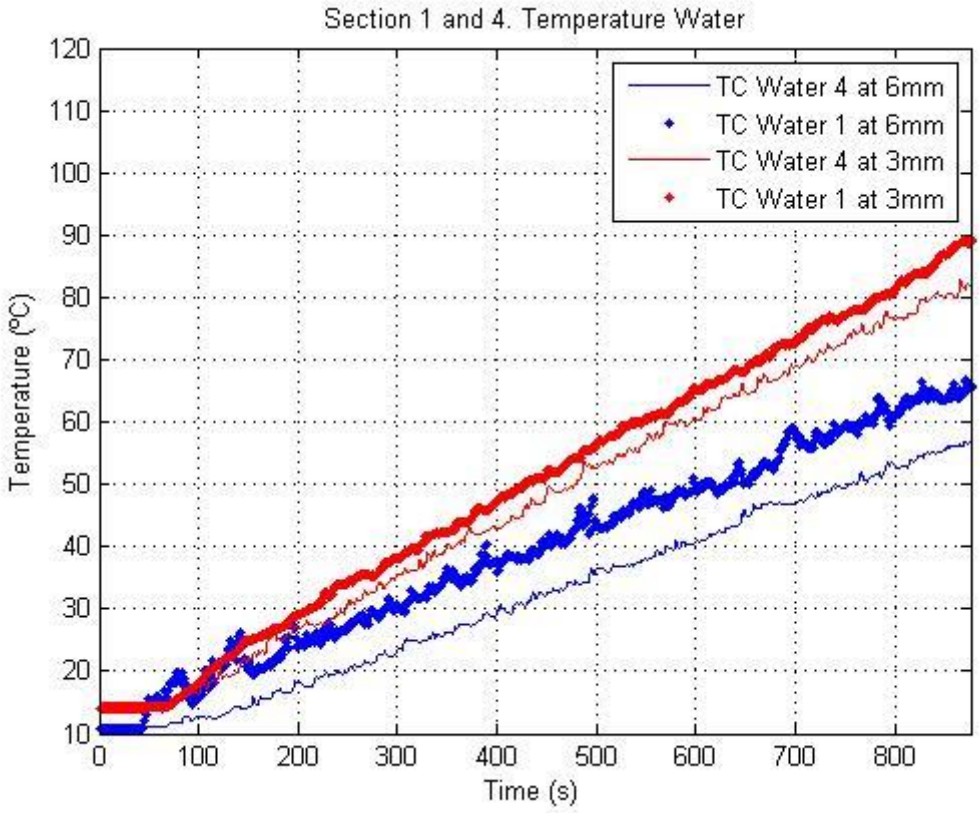

Figure 35: Experiments 4 and 5. Measurements of thermocouples at section 1 and 4 inside the tube.

As expected the temperatures of the water at section 1 are higher than the ones at section 4 in both experiments and we can clearly see that the temperature difference between both experiments is increasing progressively. This data will help us to study the temperature absorbed by the water in each experiment.

3. Cooling water measurement

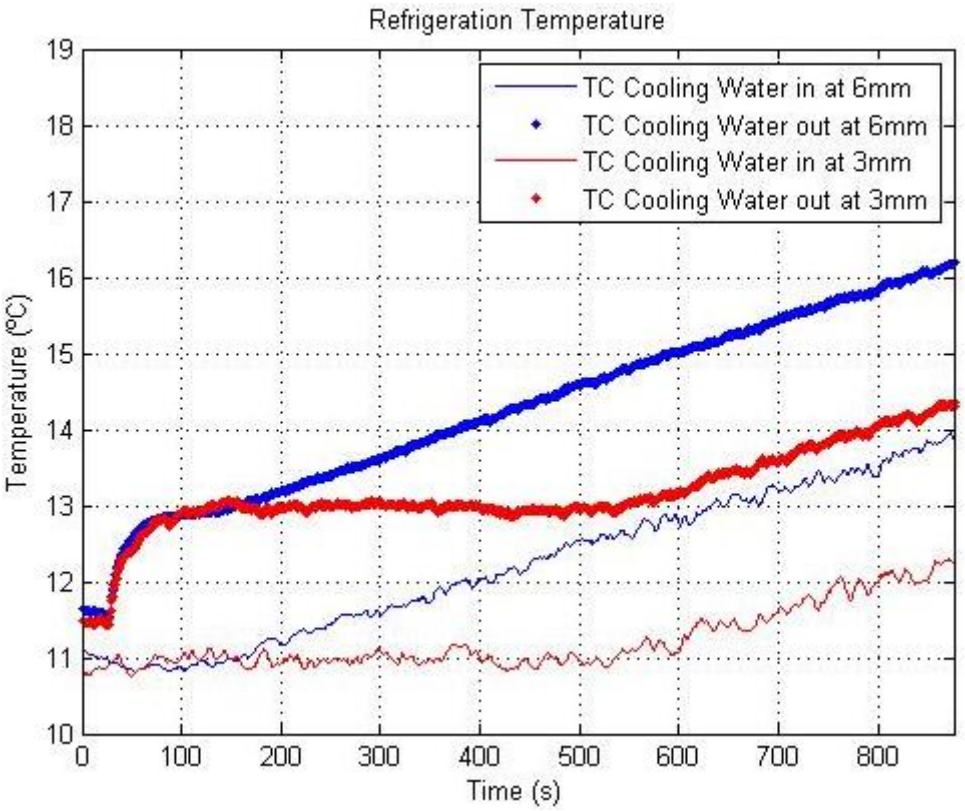

Figure 36: Experiments 4 and 5. Measurements of thermocouples at inlet and outlet of the refrigeration cycle.

As we can see for this final graph the temperature reached in the experiment of 6 mm is much higher than the one for 3 mm. These temperatures should be closely related due to fact that the inductor provides the same load. The differences presented can be caused by the different working conditions from one experiment to the other. The experiments where performed at different days and any change of the procedure could be affecting the values measured. Anyways the pattern is similar for both experiments having a constant temperature difference from the outlet to the inlet measurements.

3.5.1. RESULTS SET 2

With the data previously explained in each graph we have been able to perform the study of the heat absorbed by each consumption source.

Experiment	$\dot{Q}in$ (W)	Distance (mm)	$\dot{Q}abswater$ (W)	$\dot{Q}abswall$ (W)	$\dot{Q}ref$ (W)	$\dot{Q}lost$ (W)
4	2000	3	396,46	232,46	1115,2	255,88
5	2000	6	270,68	11,623	55,76	12,794

Table 4: Results obtained for the heat transmission.

For a better understanding of the values obtained in Table 4 a diagram of the percentage corresponding to each consumption source is provided:

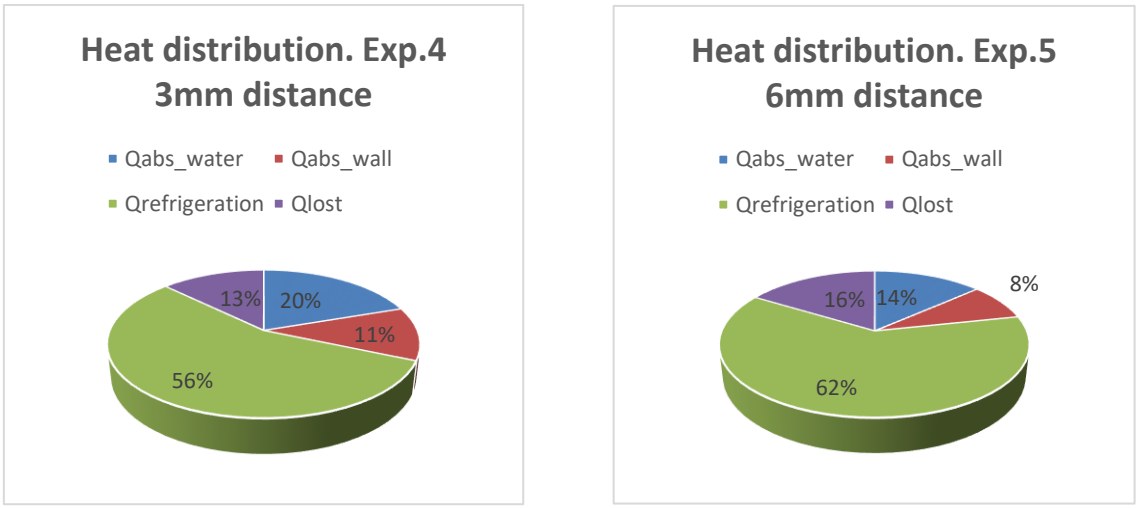

a) *b)*

Figure 37: a) Heat distribution results of experiment 4. b) Heat distribution results of experiment 5.

From the previous diagrams obtained we can clearly see that the heat absorbed by the water is reduced a 6% from the experiment at 3mm to the one at 6 mm distance, meaning that the experiment 4 has obtained a better performance. The distance of 3 mm must be used for future experiments as the manufacturer recommends.

4. CIRCULATION OF THE MOLTEN SALTS EXPERIMENT

The most important experiment achieved during the period worked with the installation was the circulation of the molten salts through the system. By this experiment we have been able to calculate the heat transfer distribution through the not isolated part of the loop where the inductor will be located in future studies. Also, the performance of the salts at different temperatures and velocities was achieved. The description of this experiment tries to give an insight of the most important results and be a guide for further research of the installation.

4.1. PREPARATION OF THE EXPERIMENT

Several experiments have been conducted variating the frequency of the pump in order to have different velocities of our heat transfer fluid inside the installation and by this be able to obtain an average value for the heat losses in the section of the tube under study.

Before going deeper on working principles of the experiment a brief explanation of the security steps must be presented. The following points try to be a safety model for future experiments and must be followed in order to avoid accidents and mistakes on the measurements:

1. Check the adequate temperature of the molten salts on the tank. For this the temperatures shown in the control box must be annotated. These temperatures correspond to:
    1. Security indicator.
    2. Thermocouple in the down part of the tank.
    3. Thermocouple in the wall of the tank.

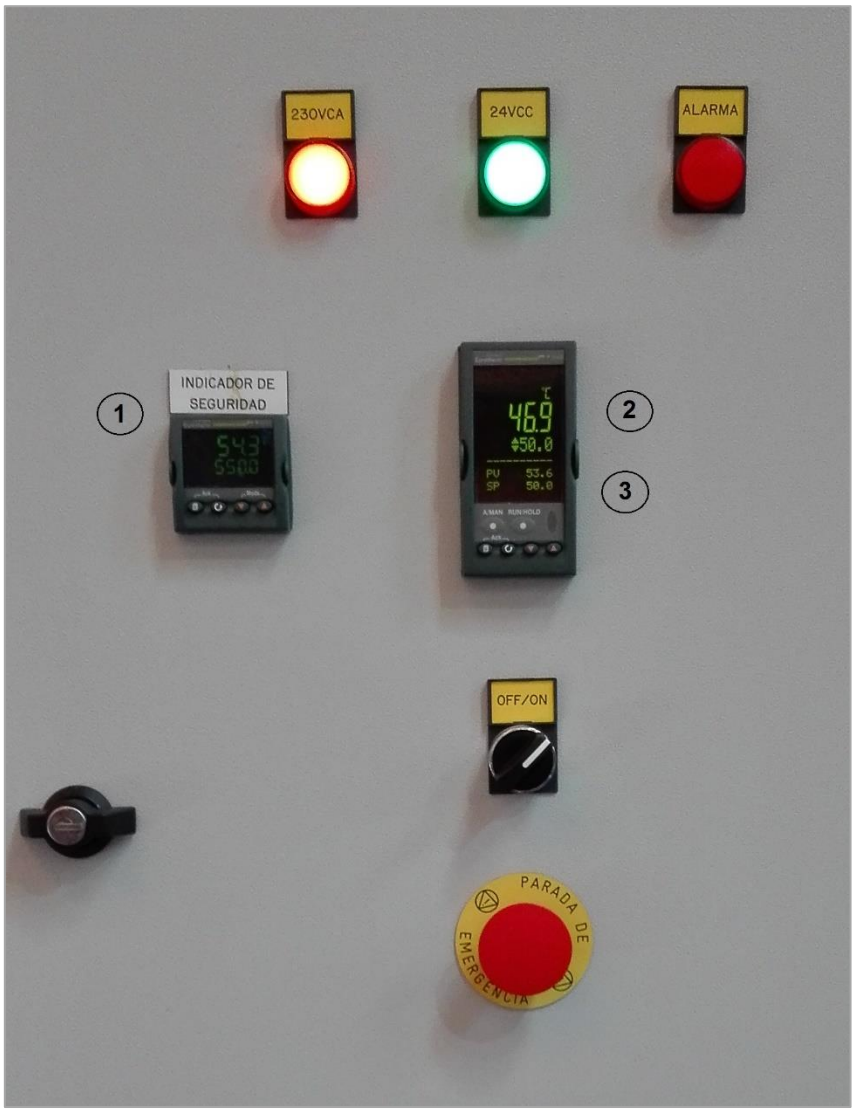

Figure 38: Control box.

2. Check the temperatures of the two trace parts that are shown in the general box. These values must be equal to the ones specified by the set points. Normally 300 °C.

3. Locate the mirrors inside the experiment room in order to be able to see the following key sections from outside the room:

    1. Section where the inductor will be located.
    2. Pump shaft.
    3. Elbow of the loop.
    4. Pressure sensor.

4. Locked the door. During the experiment is forbidden to go inside the room where the circulation is taking place.

5. Turn on the flowmeter.

6. Check that the reserve switch inside the general box is down. (Problems appeared when it was up).

7. Switch on the frequency controller.

8. Program the frequency controller following the steps summarized in Annex 2.

9. After pressing run, the pump must have started so with the help of the mirror, previously installed, we will check that the shaft is rotating and also if any problem is occurring inside the room.

10. Next step will be to check the flowmeter.

11. Check the pressure sensor.

12. Check the temperatures of the receiver.

13. Wait until the circulation is developed and repeat point 1 with also writing down the measure of the flowmeter.

For switching off the installation we will follow:

1. Press the Stop button in the frequency controller.
2. Check the inside with the help of the mirrors.
3. Check flowmeter.
4. Switch off the frequency controller in the general box.
5. Wait for 1 hour while the salts return to the tank by their own weight.
6. Turn off the trace.

4.2. EXPERIMENT CONFIGURATION

After the start of the circulation we have obtained the measurements done by the thermocouples in different locations of the tube. The position of these thermocouples has been decided for studying the heat distribution at 4 different locations of the tube close to the position where the inductor will be located. A schematic representation has been added in order to understand better the position of this measuring tools and also a picture of the real disposition is given for a better visualization:

The numbers have an ordered system being the first one the sector and the second the position in the radial coordinates.

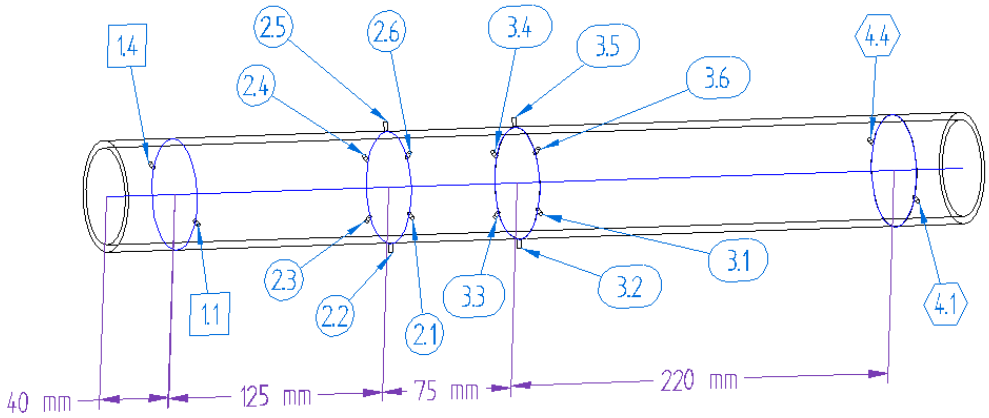

Figure 39: Location of the thermocouples in the tube.

For each section, we will have the following positioning:

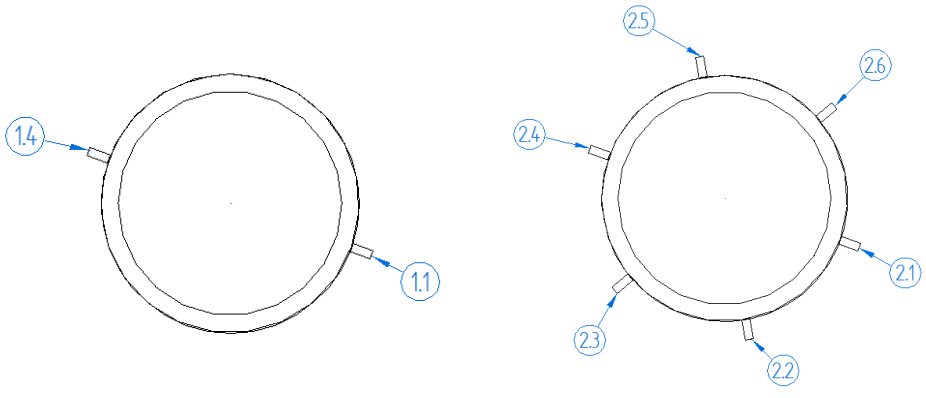

a) *b)*

Figure 40: a) Area 1 cross section. b) Area 2 cross section.

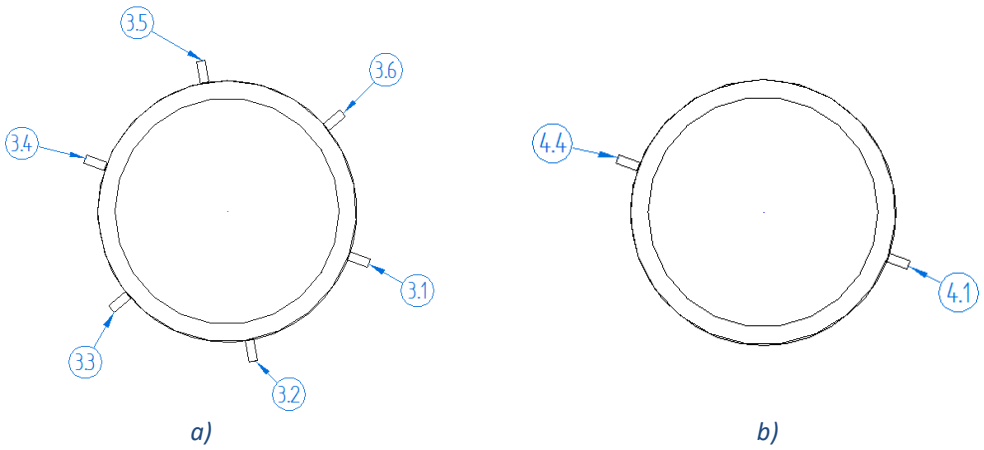

Figure 41: a) Area 3 cross section. b) Area 4 cross section.

The real disposition will be:

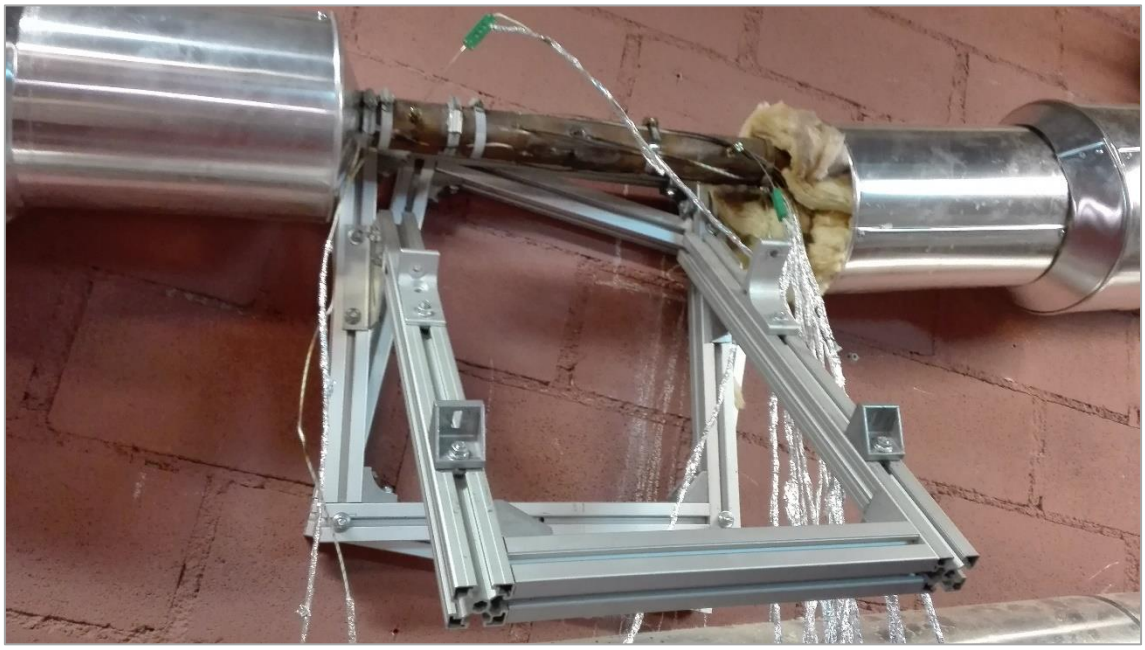

Figure 42: Section under study during the circulation experiment.

From Figure 45 we can appreciate the real section where the inductor will be applied along with its support.

With the data obtained from the thermocouples we have been able to estimate the temperature distribution in the tube section where the inductor will be connected using the software Matlab. By this we are able to approximate the heat losses produced and study the temperature changes in the different locations of the tube.

We have studied different frequencies of the pump for varying the mass flow of the molten salts setting the frequency values as explained in Annex 2.

4.3. EXPERIMENTS

On the following table, there are summarized the experiments performed during the study. Other experiments have been conducted but without recording relevant data since these experiments were the first ones conducted and the objective was the circulation of the molten salts and not the measurements of the thermocouples.

Experiment	Time (min)	Frequency (Hz)	Velocity (m/s)	T_INF/T_ALARM (Security Indicator) (°C)	Temp. Salts inferior/T_SP (°C)	Temp. Salts Wall T_PV/ T_SP (°C)
1	10	10	1,10	449/550	447/350	450/350
			1,12	438/550	438/350	437/350
2	10	20	2,24	436/550	430/350	436/350
			2,23	427/550	426,4/350	425/350
3	10	10	1,2	478/550	472/480	480/480
			1,19	471/550	468/480	480/480
4	10	15	1,77	460/550	460/480	480/480
			1,76	458/550	455/480	476/480
5	10	20	2,36	457/550	454/480	475/480
			2,35	456/550	451/480	471/480
6	10	10	1,09	423/550	420/350	422/350
			1,08	416/550	416/350	415/350
7	10	20	2,26	462/550	460/350	461/350
			2,27	450/550	450/350	450/350

Table 5: Circulation experiments.

As we can see from Table 5 the experiments have different frequencies and start at different temperatures in order to evaluate the accuracy of the data obtained in terms of similarity and resulting in the achievement of logical results. The only experiments studied are the first and the second, which are pointed out in the table. This is due to the similar results obtained for the rest of the experiments.

As shown on the table each experiment is done during an interval of 10 minutes with the main variant of different frequency of the pump and different initial temperature due to heat losses during the circulation. Could not be understood that for the same frequency the molten salts achieve different velocities but this fact can be explained by understanding that the initial temperatures are different for each experiment. This variable should be corrected in future experiments for reaching conclusions about the errors in the velocity.

The temperature values shown on the three last columns of the previous tables correspond to the data obtained by the thermocouples located on the different heights of the tank as shown on the following explanation diagram.

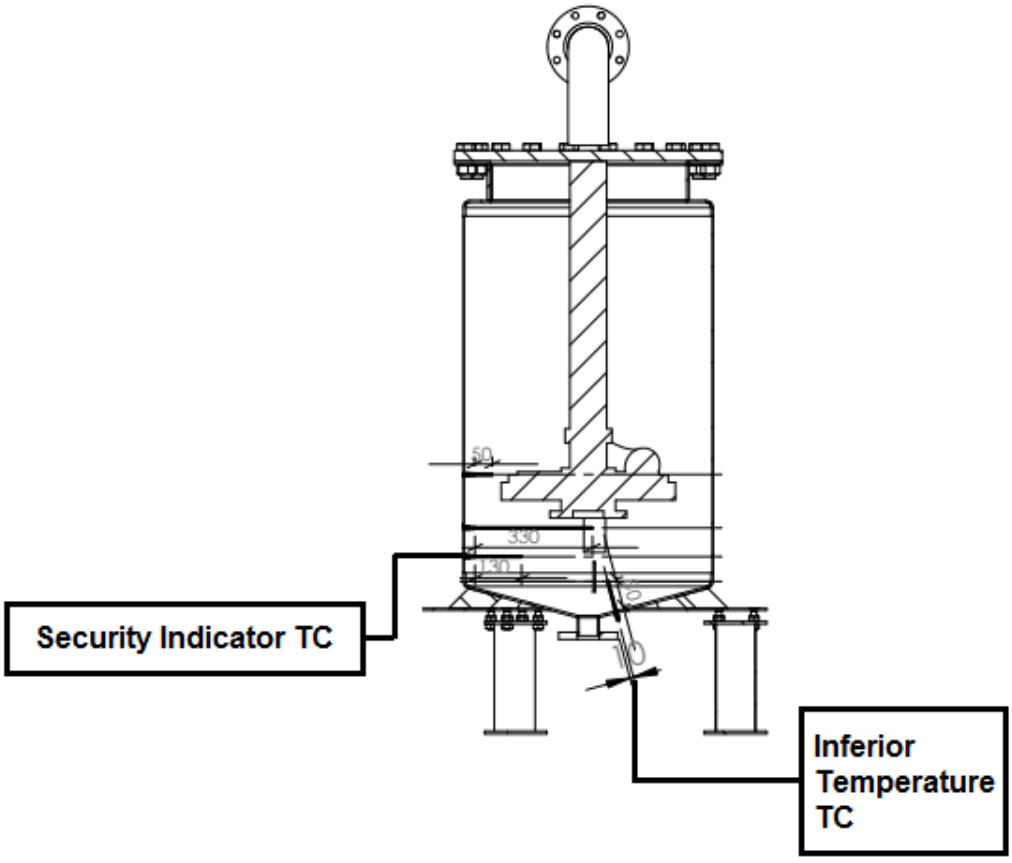

Figure 43: Thermocouples located at the storage tank.

From Figure 39 we can appreciate the location of the thermocouples located at the tank. These values are displayed in the control box as we have already appreciated in Figure 38 but for the thermocouple located at the wall of the tank which is not appreciated from this figure.

4.4. RESULTS

The experiments mentioned before consisted on the circulation of the molten salts trough the circulation loop at different rotational frequency of the pump and also at different temperatures of initialization. For the different experiments, the values obtained from the thermocouples at the walls and inside the tubes previously explained will be given along with the calculation of the heat losses during the process.

4.4.1. EXPERIMENT 1

As explained in the preparation of the experiment section the first step of the experiment was following the security steps and select the rotational frequency of the pump. On the table of the experiments we can see that for 10 Hz, and at the conditions of the salts at that moment, the velocity marked by the flowmeter was 1,09 m/s. For this velocity and the conditions of the salts we have obtained the following temperature distribution for each section of measurements:

At the moment the experiment was performed, the thermocouple located at section 1 position 1 did not read properly so the results shown on the next figure are only for the three left available measurements.

1. Section 1 and 4

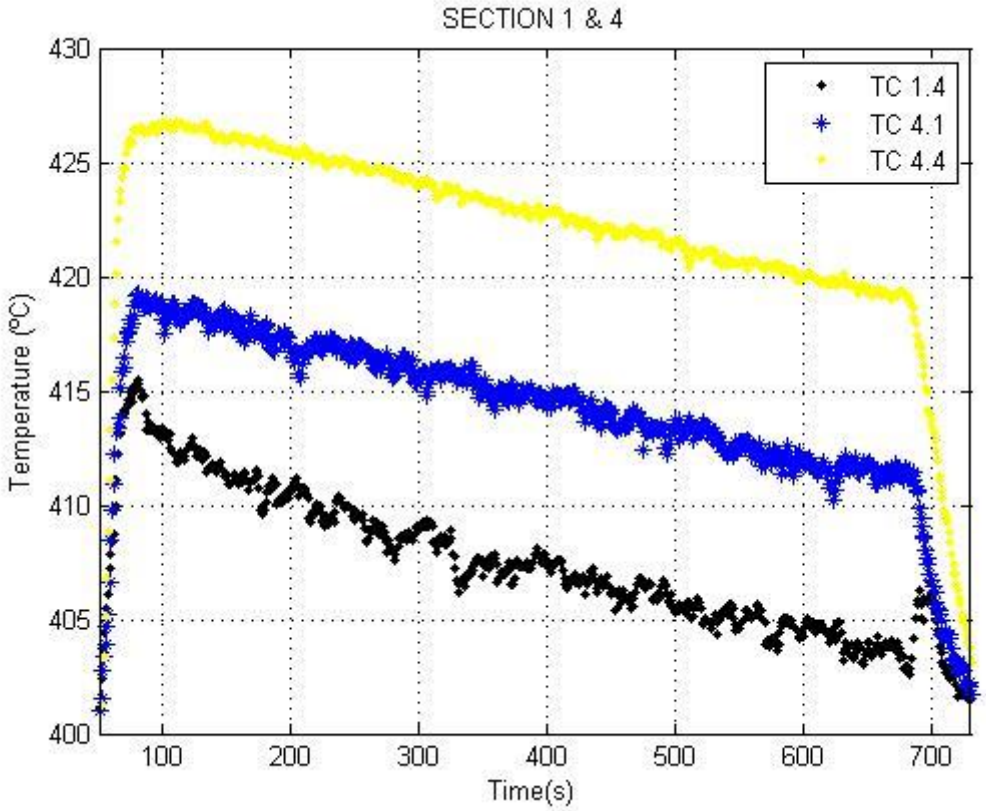

Figure 44: Temperature measured by section 1 and 4 thermocouples. Exp.1.

As we can see from the results obtained the temperature is higher at the measurements of the thermocouples located at section 4, something not totally understood because the expected results were a higher temperature at section 1 where the temperature losses produced by the lack of insulation are lower than at section 4.

The temperature difference is of 5 °C from one measurement to the other, something understandable maybe for different sections but not for the same section. The difference between measurements 4.4 and 4.1 is larger than expected. Because of this, special consideration will be taken in the following pages to the measurements of the thermocouples at these positions.

2. Section 2

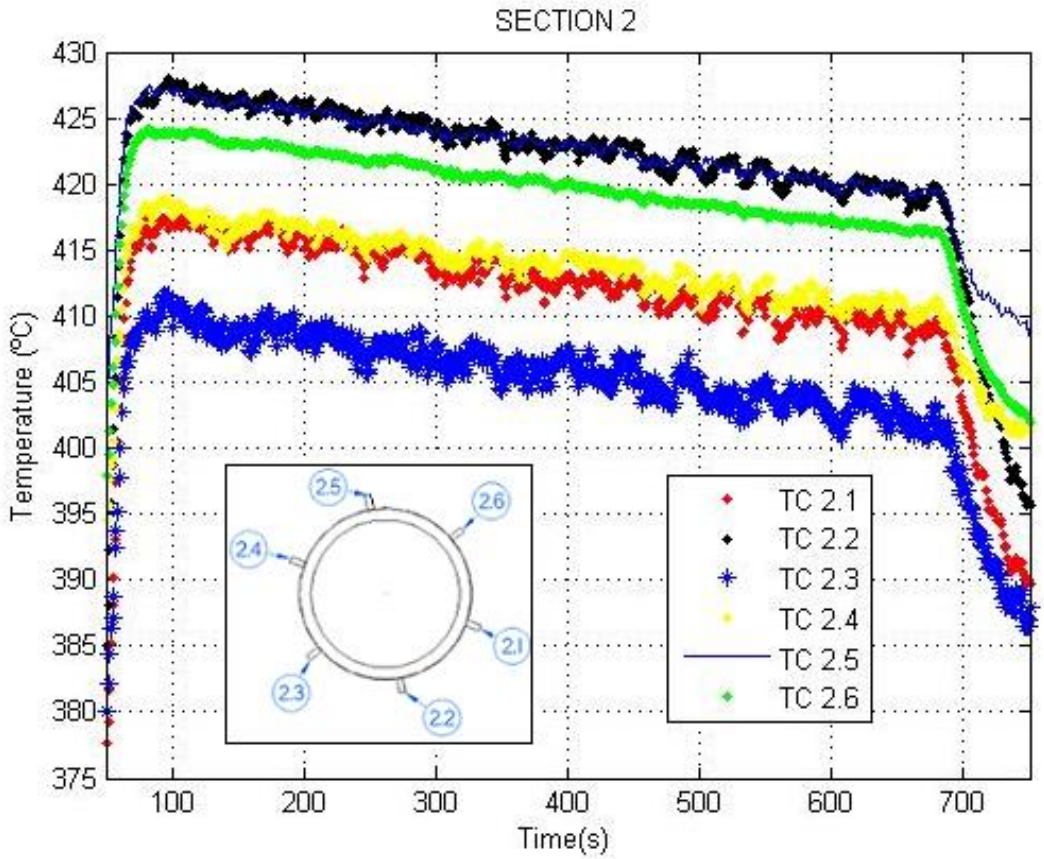

Figure 45: Temperature measured by section 2 thermocouples. Exp. 1.

For section 2 we can see that the highest temperature values correspond to the thermocouples located at position 2 and 5 followed by 6, 4 and 1 closely related and finally 3. These high jumps of temperature from one location to the rest need a further study because there was not expected a difference of around 17 °C from the warmest to the coolest measure.

Comparing this results with the previous obtained at section 4 we can see that the pattern is not repeated with respect the locations 1 and 4. On the previous graph we could see a different temperature of around 5 degrees while on section 2 the temperature of 4 and 1 are similar with a slightly higher value for location 4.

3. Section 3

For the experiment of section 3 we only have measurements for 5 locations instead of the 6 expected due to technical problems with the thermocouple located at section 3 point 1.

We have obtained the following results:

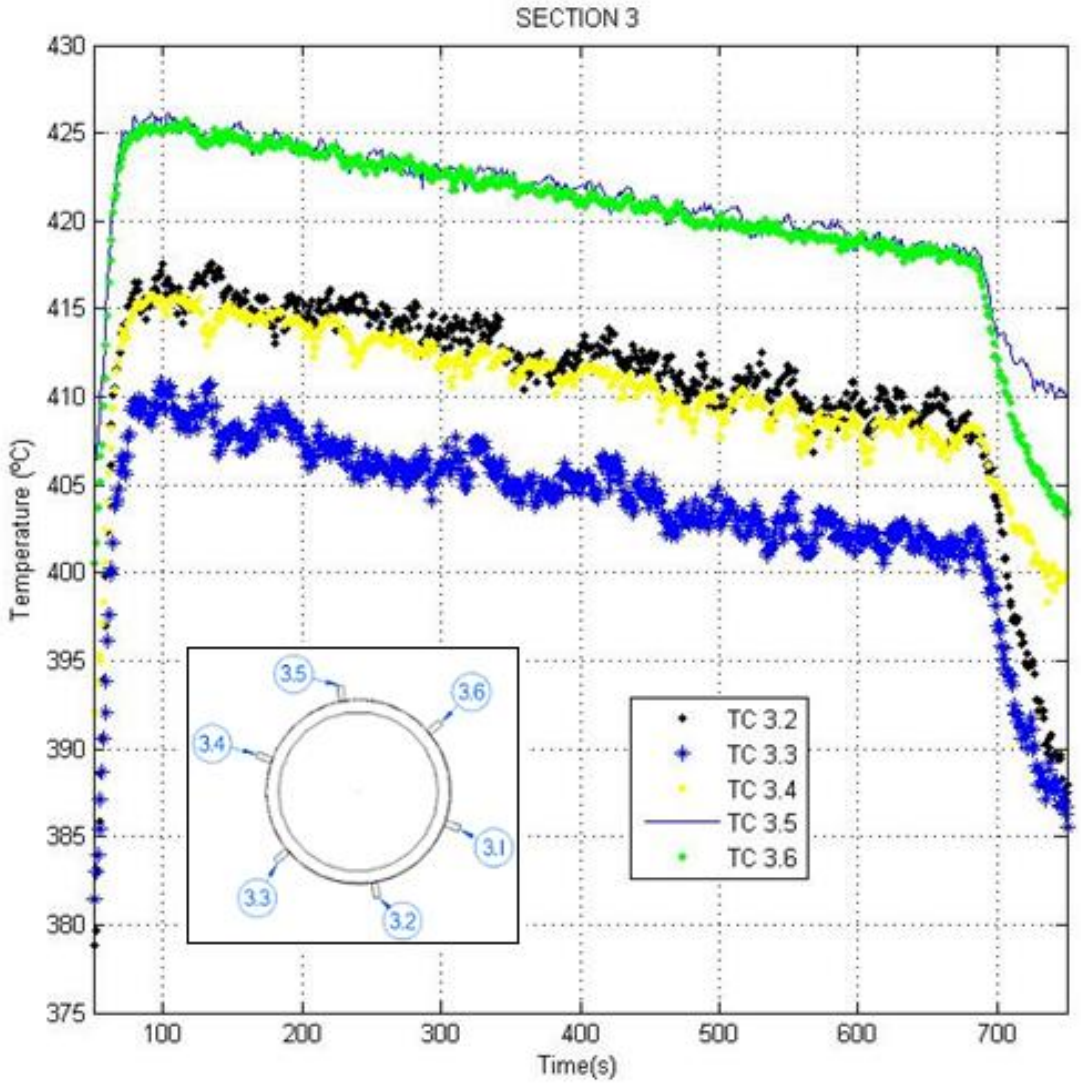

Figure 46: Temperature measured by section 3 thermocouples. Exp. 1.

For section 3 the temperatures at the different locations can be expressed in a decreasing pattern as (3.5 and 3.6) > (3.2 and 3.4) > 3.3. Comparing the results with the previous obtained we can say that the temperature pattern is similar with maximum temperatures around 426 °C and lowest around 410 °C but these temperatures are not recorded for the same positions. While at section 2 the highest temperatures were recorded by 2.2 and 2.5 followed by 2.6, for section 3 the maximum temperatures correspond to 3.5 and 3.6 something more understandable due to its proximity but the

position 3.2 does not even reach 420 °C while before its temperature reached 426 °C at the beginning of the circulation.

These strange results made us consider that the thermocouples located at section 2 or either at section 3 were not well positioned but after a verification experiment of each thermocouple we checked that all of them where measuring at their expected position. This verification left us more interrogates than answers making a matter of study for future experiments the different measurements recorded from section 2 and 3 which are separated only by 75mm.

4. Temperatures in section 1 and 4 inside the tube

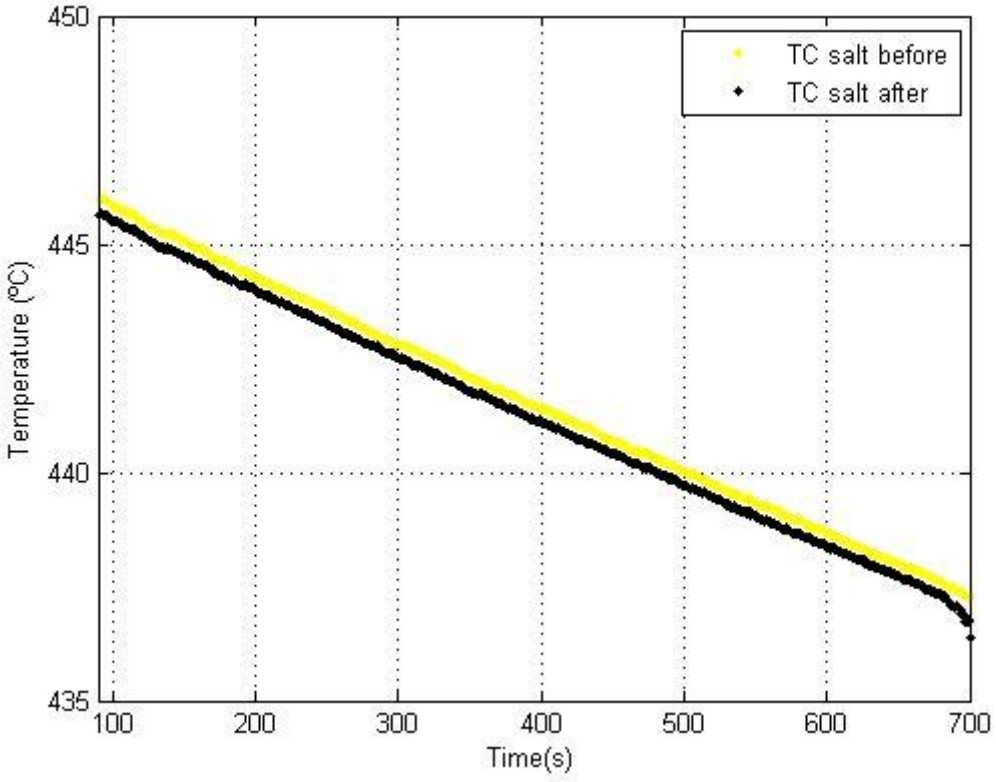

Figure 47: Temperature of the molten salts in section 1 and 4.

With this graph, we can see that the temperature inside the tube does not variate a lot from section 1 to section 4 which means that the heat losses will be low. As expected the temperature at section 1 is slightly higher than the one a section 4, something understandable taking into account the losses produced through the not isolated section.

5. Tank

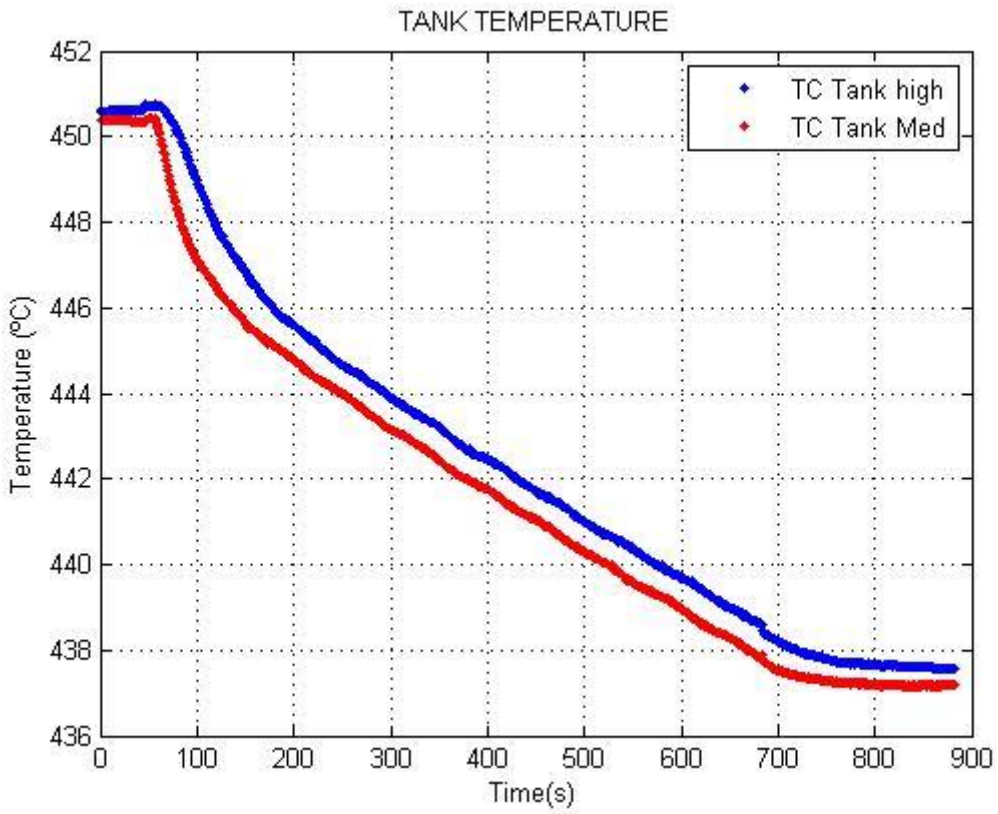

Figure 48: Temperatures of the tank at two different heights.

On the previous figure the temperature development of the molten salts is accounted from the point of view of the tank, where two thermocouples are located. TC Tank high corresponds to the Wall Temperature TC while TC Tank Med corresponds to the Security Indicator TC, the location of this last thermocouple is shown on Figure 39. As we can see the temperature decreases while operating the experiment and is maintained constant when the circulation process is off, this provide us a better understanding of the heat losses produced during the circulation.

4.4.2. EXPERIMENT 2

This experiment was performed right after the previous study explained. As shown in the experiments table the velocity of the salts for a rotational frequency of 20 Hz corresponded to 2,24 m/s at the given temperature conditions.

1. Section 1 and 4

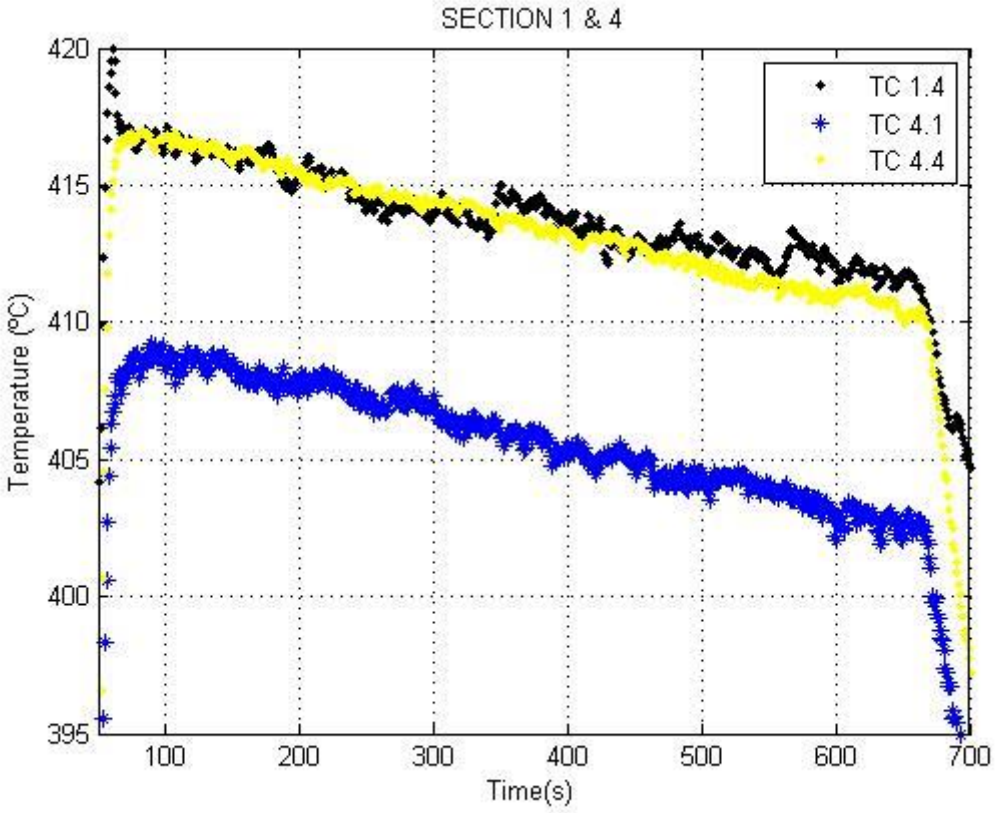

Figure 49: Temperature measured by section 1 and 4 thermocouples. Exp. 2.

From Figure 49, we can see that the temperatures for section 1 and 4 are equal for point 4 and inside section 4 we can distinguish a 5°C drop from point 4 to point 1. This last difference was recorded also in the previous experiment. Also, we can see that the temperature ranges are lower due to the heat losses developed from the end of one experiment to the beginning of the other.

It is interesting the fact that the temperature at section 1 now has a similar value than the one at section 4 while in the previous experiment there were around 10 °C difference. This change is continuous as we checked in other experiments where from the first experiment performed to the last the temperature at section 1 increased gradually with respect to the one at section 4.

2. Section 2

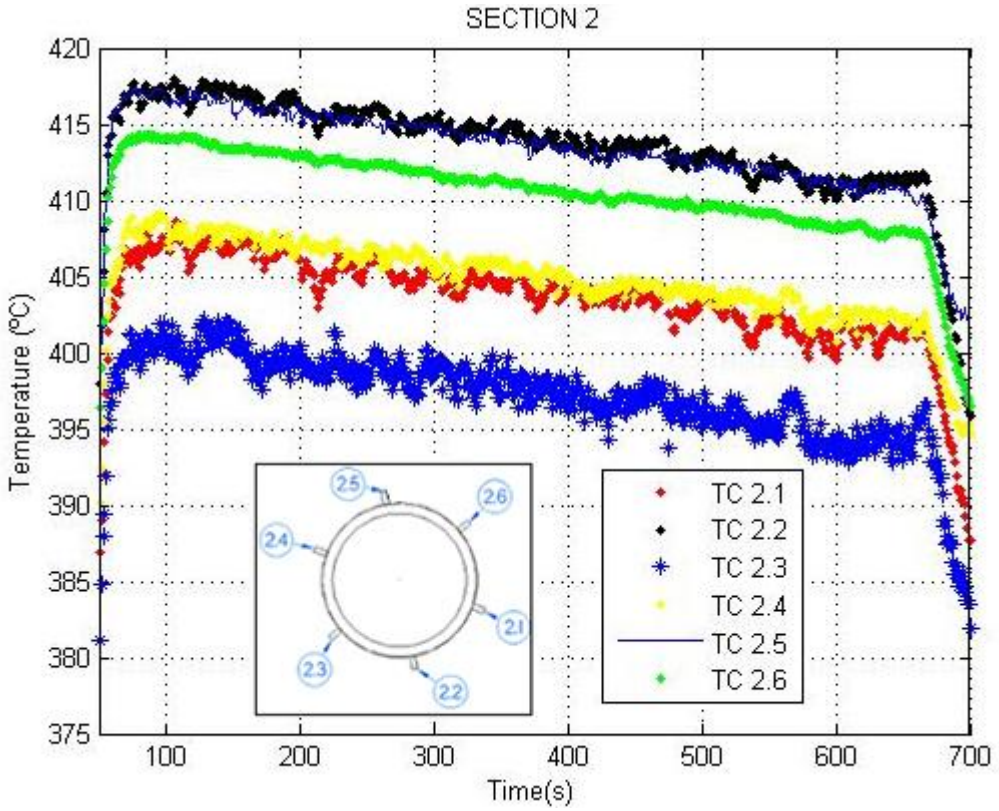

Figure 50: Temperature measured by section 2 thermocouples. Exp. 2.

For section 2 we can distinguish that the highest temperatures correspond to location 2 and location 5 followed by a gap of 3 °C by point 6, then point 4 and 1 closely related and ending the list with point 3 with a difference of around 17°C from the leading values. The pattern is similar to the one already observed in the previous experiment for the same section.

3. Section 3

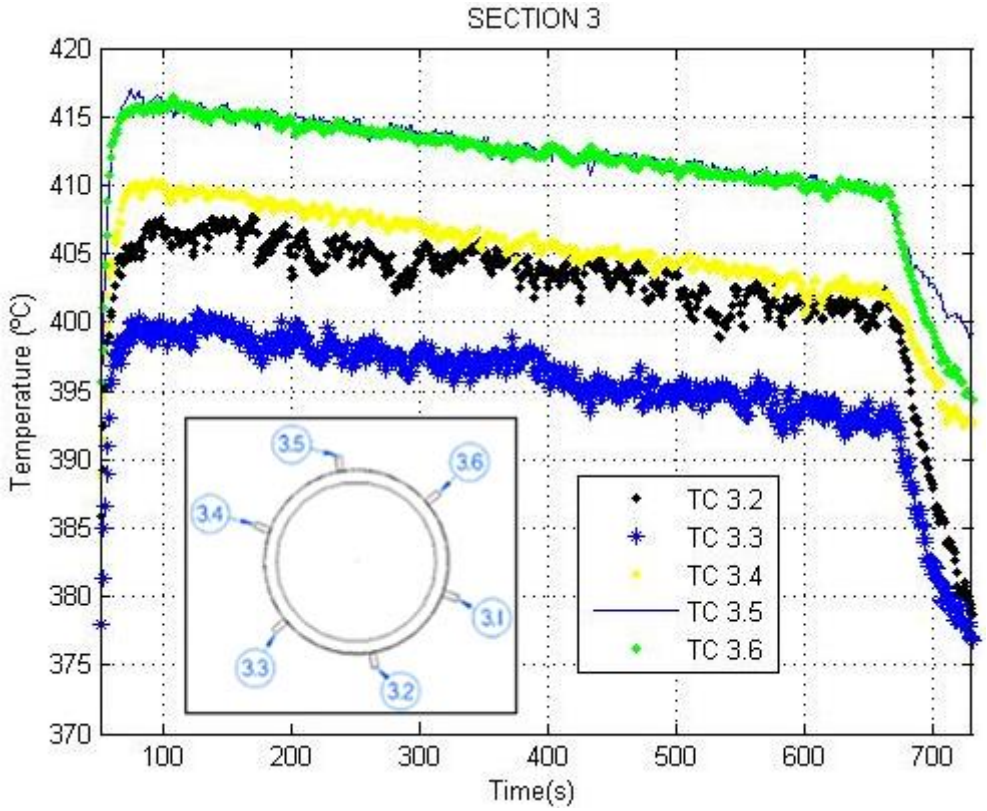

Figure 51: Temperature measured by section 3 thermocouples. Exp. 2.

From this last graph, we can see how the thermocouples at points 5 and 6 measure similar values with around 415°C at the beginning of the circulation while points 4, 2 and 3 mark lower values as 410, 408 and 400 °C respectively.

Comparing these results to section 2 we can see as common feature the point 3 as the lowest value and point 5 as the highest for both section with point 4 in a middle position while the other thermocouples performed different patterns. At the end of this section a separate study of section 2 and 3 will try to clarify the differences between both measurements.

4. Temperatures in section 1 and 4 inside the tube

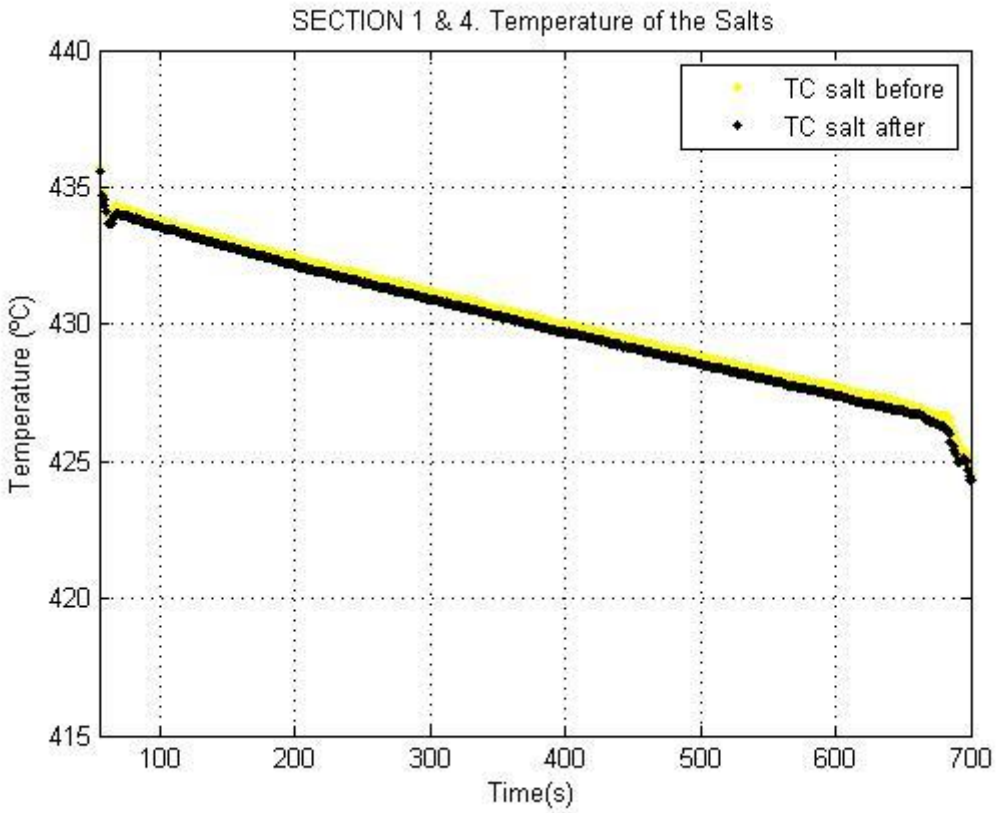

Figure 52: Temperature of the molten salts in section 1 and 4.

As viewed on the previous experiment the temperature of the salts decreases progressively but without a big difference between the two sections. We have to mention that the fact that the temperature in section 1 is greater than in section 2 is again the expected result when from section 1 to section 4 exist heat losses due to the lack of insulation material.

5. Tank

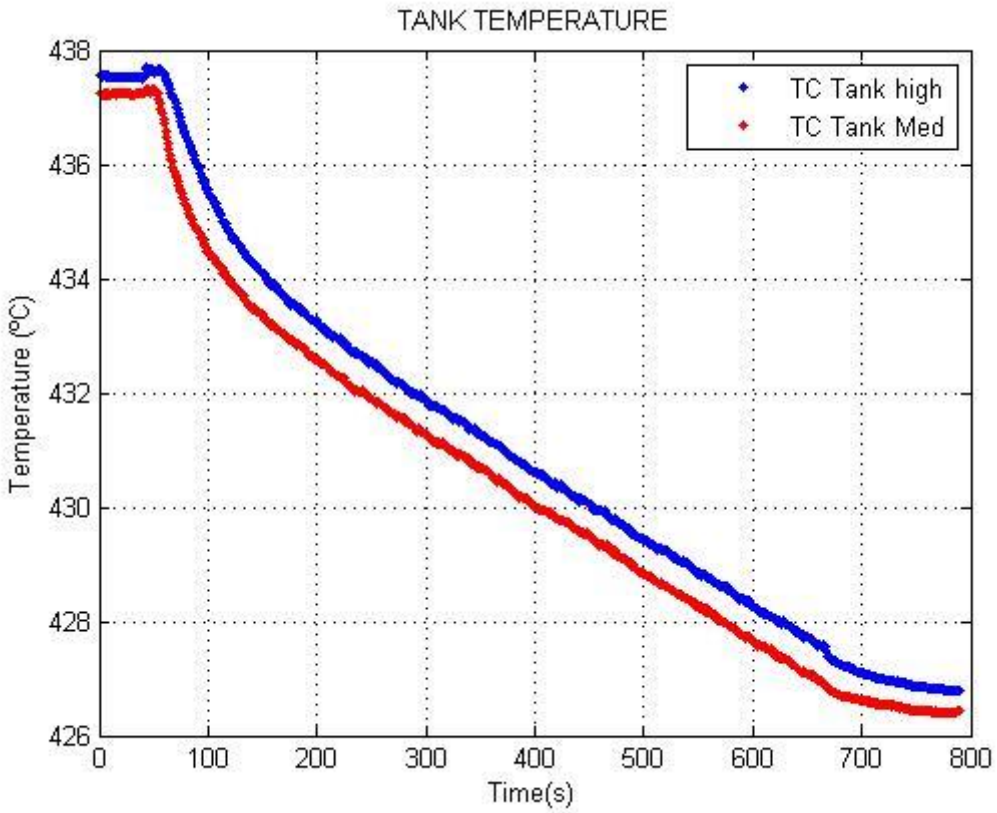

Figure 53: Temperatures of the tank at two different heights.

As before the temperature of the tank is reduced during the circulation process with lower values in the medium part of the tank than in the higher part. This temperature difference is less than 1 °C and is caused by the tendency of fluids of trying to reach higher layers when their temperature increases. The pump could affect this temperature difference if we were working with another heat transfer fluid as water.

4.4.3. COMPARISON AND RESULTS

For clarifying the performance shown at section 2 and section 3 the temperatures measured at an instant of time will be studied for both experiments. The instant selected is the second 400.

	Experiment 1. 10 Hz.			Experiment 2. 20 Hz.		
	Section 2 (°C)	Section 3 (°C)	Variation |ΔT| (°C)	Section 2 (°C)	Section 3 (°C)	Variation |ΔT| (°C)
Position 1	412,8	-	-	404,9	-	-
Position 2	423	412,5	10,5	414,4	402,5	11,9
Position 3	407,3	405,5	1,8	396,1	395,6	0,5
Position 4	414,7	411,4	3,3	404,5	405,5	1
Position 5	423,3	422	1,3	413,2	412,7	0,5
Position 6	420	421,2	1,2	410,1	412,8	2,7

Table 6: Test for the thermocouples at section 2 and 3.

From the previous table, we can see the temperature values recorded at the 400 second at section 2 and 3 along with their absolute differences for both experiments. From this we can conclude that the temperature values are similar in both sections, as we expected due to the short distance between the two sections (75 mm), but for the measurements of point 2 which as we can see measures a variation from one section to the other of 10,5 °C for the first experiment and 11,9 °C for the second one. These differences are not expected, as we already explained during the experiments, and we consider that the temperature measurements are especially strange for the thermocouple at section 2 and position 2 which is the thermocouple measuring higher values. This assumption is done in the basis of the values recorded next to point 2 which correspond to point 1 and point 3 of both sections and have more similarity between them.

We consider that the cause of the high measurements recorded at point 2 is the electrical heat tracing. The short heat tracing is positioned in a line of the tube and not as the long heat trace which surrounds the tube while it advances. We assume that the short heat trace is affecting the measures of section 2 point 2 because it is positioned in the same line. Due to this fact in future experiments the researches should reconsider the installation of the short heat tracing in a different way for distributing better its temperature.

On the following table, we can see the results obtained for the circulation of the molten salts experiment:

	Experiment 1. 10 Hz	Experiment 2. 20 Hz	Units
Heat transfer (Q)	1756,7	3026,3	W
Average temperature difference from section 1 to section 4 (ΔT)	0,30	0,26	(°C)
Average mass flow ($\dot{m}$)	3,84	7,71	kg/s
Reynolds number (Re)	62261	120410	-

Table 7: Results obtained for the molten salts circulation experiment.

From the previous results, we can clearly see that the experiment at higher velocity is the one with higher heat losses due primarily to the increase of mass flow of the thermal fluid. As we could observe from Figures 49 and 54 the temperature change in the section where the inductor will be located is similar in both experiments and very low.

For the Reynolds numbers obtained we must mentioned that the experiment at lower frequency is the one that is more approximated to the normal conditions of a CSP plant where the order of maximum values is of $5 * 10^4$. For future experiments a lower frequency should be imposed in order to approximate better the velocities obtained inside of the tube.

5. CONCLUSION

On this last part of the project a feedback of the performance of the installation during the project is exposed along with a summary of the most relevant results obtained.

While advancing with the commissioning of the experiments some troubles appeared making the process slower. For example, after having results using the inductor machine with the tube filled with water another experiment was performed at higher inductor load resulting in the burning of the flux concentrator. This part of the inductor was sent to be repaired but when it appeared that the manufacturers have fixed the problem and we tried for the second time higher inductor loads than 3KW the same problem appeared. At the end of this report composition the manufacturers did not have delivered the final device.

One of the positive achievements while working on the project was the performance of the experiment regarding the circulation of the molten salts through the cycle. May appear as a simple step but there were a lot of concerns at the beginning. Before the circulation of molten salts only water had been use in the circulating process given good results in terms of the pump and on some measurements performed by the thermocouples, but the use of molten salts implied a working temperature of around 500 °C which could have result in damage for the installation or even safety problems.

The two set of experiments shown on this final project are able to approximate a little closer the final objective of the installation of performing simultaneously the circulation of the salts and the appliance of the inductor machine. Once this final experiment will be performed deeper understanding of the functioning of a central receiver will be achieved and hopefully results for improving the efficiency of CSP plants.

The objectives marked at the beginning of this project have been achieved with better results than expected in some cases but with the negative feature of not being able to perform the experiment previously explained due to lack of time.

About the knowledge goal I can say that I have learnt about the solar thermal power field and I am able to defend it better than at the beginning. In relation with the installation I have worked with it and learn about it and the best proof are the experiments conducted on my own for the circulation of the molten salts.

The commissioning of the experiment objective is justified by the results obtained which in turn have permitted the calculations shown on the experiments section where we have obtained the heat transfer results for different procedures.

The critical view of the results has given us some unexpected values that will need further study, but in general the results can be said to be positive and are ready to be used in further researches.

6. FUTURE PERSPECTIVES

As already explained the main experiment is yet to be done and this will imply that finally the commissioning is over and the study can advance towards the next step of obtaining valuable data corresponding the simulation of a central receiver. These achievements will possibly be reached by the end of this year and hopefully without any new inconvenient. The steps to follow will mainly be the allocation of the inductor machine in the section of the upper tube without insulation and surrounded by the thermocouples already explained in the circulation experiment. After this step, new experiments will be done varying the load provided by the inductor as well as the mass flow of the molten salts inside of the tubes as we have performed separately during the period worked with the installation. By changing these parameters, the real characteristics of a solar thermal power plant will be simulated and the installation will be operative for further studies, becoming one of the most interesting experiments in the field.

By widening the perspective, we can say that the future of thermal power plants is promising and efforts like the one performed for achieving this project should be repeated in other countries and even with more ambitious goals. The investment toward cleaner energies should be a matter of discussion because the whole society directly or indirectly is affected and even if this project could seem a small step toward an energy transition it could also mean the motivation for another study or even the final results could be adopted by commercial power plants. As already explained there are already in the world 23 new plants under construction and with an increase of efficiency this number could be multiplied and obtain and important share in the global energy mix.

7. ANNEXES

7.1. ANNEX 1: Property tables

1.1

Molten Salts Properties for Tsalts (ºC)		
Properties	Values	Units
Density (ρ)	$2090 - 0{,}636 * Tsalts$	$\frac{Kg}{m^3}$
Specific heat (Cp)	$1443 + 0{,}172 * Tsalts$	$\frac{J}{Kg * °C}$
Thermal conductivity (K)	$0{,}443 + 1{,}9 * 10^{-4} * Tsalts$	$\frac{W}{m * °C}$
Viscosity (μ)	$22{,}714 - 0{,}120 * Tsalts + 2{,}281 * 10^{-4} * Tsalts^2 - 1{,}474 * 10^{-7} * Tsalts^3$	mPa*s

Table 8: Molten Salts Properties [45].

1.2

Tube AISI 316		
Properties	Values	Units
Density	7,99	$\frac{g}{cm^3}$
Specific heat	0,5	$\frac{KJ}{Kg * K}$
Thermal conductivity (at 500ºC)	21,4	$\frac{W}{m * K}$
External diameter	60	mm
Internal diameter	52	mm

Table 9: Stainless Steel Properties [46].

1.3

Properties of the resistance located at the base of the tank	
Panel Heater	Units
Dimensions	0,47*0,47 m
Heater	0,4*0,45 m
Thickness	0,125 m
Nº of Resistance	1
Total Power	3 KW
Voltage	230 V
Maximum Temperature	1300 °C

Table 10: Base Resistance of the tank [47].

1.4

Properties of the resistance located at the wall of the tank	
Semi cylinders heaters	Units
Internal Diameter	0,76 m
Exterior diameter	1,01 m
Length	0,6 m
Thickness	0,125 m
Angle	180º
Nº of resistance	4
Total power	12 KW
Voltage	230 V
Maximum Temperature	1300 °C

Table 11: Wall Resistance of the tank [47].

1.5

Circulation pump properties	
Weight	300 kg
Motor velocity	1500 rpm
Nominal Power	37 KW
Motor working frequency	50 Hz

Table 12: Circulation pump properties.

1.6

Induction machine water needs	
Consumption, min.	10 l/ min
Water inlet temperature	35 °C
Water minimum pressure difference in-out	4 bars
Water maximum pressure difference in-out	6 bars

Table 13: Induction machine cooling water needs.

1.7

Electric heat tracing	
Maximum Temperature reached	550 °C
Ambient temperature Min/Max	0 °C / 40 °C
Power source	230 Vac FNT-50Hz
Maximum exposition temperature	1000 °C
Maximum working tension	600 V

Table 14: Electric heat tracing properties [40].

7.2. ANNEX 2: Circulation of the molten salts devices configuration

Connection of the electrical heat tracing
1. Control panel
2. Rise automatic trace switch
3. Rise short and long traces switch
4. Stablish set point for the temperature of the electrical heat tracing. Button “P”

Table 15: Connection of the heat tracing system.

Figure 54: Heat Tracing switches.

Frequency controller configuration
1. Rise frequency controller switch.
2. On the screen will appear: POTF 0.00 Hz
3. Press ESC button.
4. Press down arrow until “PARA” is shown on the screen.
5. Press Enter.
6. Press down arrow until “418” is shown.
7. Press Enter.
8. Select desire frequency.
9. Press Enter.
10. Press ESC until the menu: VAL/PAL is shown.
11. Press Stop.
12. Press Run.

Table 16: Frequency controller configuration.

Figure 55: Frequency controller.

7.3. ANNEX 3: Formulas used during the induction experiment

Formula 1. Heat transferred to the refrigeration system $\dot{Q}ref = \dot{m}ref * Cpwater * (Tref.outlet - Tref.inlet)$		
Concept	Formula	Value
$\dot{m}ref$	$\dot{V}ref * \rho water$	$0{,}137\ \frac{kg}{s}$
$Cpwater$	-	$4180\ \frac{J}{Kg * °C}$
$Tref.outlet$	-	Measured by a thermocouple
$Tref.inlet$	-	Measured by a thermocouple

Table 17: Heat transferred to the refrigeration cycle formula.

Formula 2. Heat absorbed by the water $\dot{Q}abswater = mwater * Cpwater * (\frac{dTwaterinside}{dt})$		
Concept	Formula	Value
$mwater$	$Aint * hwater * \rho water$	$1{,}1kg$
$Cpwater$	-	$4180\ \frac{J}{Kg * °C}$
$\frac{dTwaterinside}{dt}$	-	Measured by the thermocouples at section 1 and 4 inside the tube.

Table 18: Heat absorbed by the water inside of the tube formula.

Formula 3. Heat absorbed by the tube wall $\dot{Q}abswall = mwall * Cpwall * (\frac{dTwall}{dt})$		
Concept	Formula	Value
$mwall$	$(Aext - Aint) * hwall * \rho water$	5,9 kg
$Cpwall$	-	$4180 \frac{J}{Kg * °C}$
$\frac{dTwall}{dt}$	-	Measured by the thermocouples at the exterior wall of the tube.

Table 19: Heat absorbed by the tube wall formula.

7.4. ANNEX 4: Matlab code

- This code corresponds to the experiment using the inductor.

```
clear; clc; close all
fileID = fopen('datos_27_03_agua_calen_zona_1_6mm_secu_11.lvm');
T_pot_10_vel_0_3mm_tube=textscan(fileID,'%f %f %f %f %f %f %f %f %f %f
%f %f %f %f');
fclose(fileID);


t_vel_0_3mm_tube=T_pot_10_vel_0_3mm_tube{1};
TC_1_1=T_pot_10_vel_0_3mm_tube{2};
TC_1_4=T_pot_10_vel_0_3mm_tube{3};
TC_2_1=T_pot_10_vel_0_3mm_tube{4};
TC_2_4=T_pot_10_vel_0_3mm_tube{5};
TC_3_1=T_pot_10_vel_0_3mm_tube{6};
TC_3_4=T_pot_10_vel_0_3mm_tube{7};
TC_4_1=T_pot_10_vel_0_3mm_tube{8};
TC_4_4=T_pot_10_vel_0_3mm_tube{9};
TC_Water_4=T_pot_10_vel_0_3mm_tube{10};
TC_Water_1=T_pot_10_vel_0_3mm_tube{11};
TC_Water_ref_in=T_pot_10_vel_0_3mm_tube{12};
TC_Water_ref_out=T_pot_10_vel_0_3mm_tube{13};
V_tube=T_pot_10_vel_0_3mm_tube{14};




figure(1)
hold on
% plot(t_vel_0_3mm_tube,TC_1_1_vel_0_3mm_tube,'r')
plot(t_vel_0_3mm_tube,TC_1_4,'.')
plot(t_vel_0_3mm_tube,TC_4_1,':')
plot(t_vel_0_3mm_tube,TC_4_4,'-.')


title('Wall Temperatures')
xlabel('Time (s)')
ylabel('Temperature (°C)')
grid on
box on

axis([0 876 0 140])


legend('Temp.Wall.1.4','Temp.Wall.4.1','Temp.Wall.4.4')

figure(2)
hold on

plot(t_vel_0_3mm_tube,TC_2_1)
plot(t_vel_0_3mm_tube,TC_2_4,'.')

title('Wall Temperatures')
```

```
xlabel('Time (s)')
ylabel('Temperature (°C)')
grid on
box on

axis([0 876 0 130])

figure(3)
hold on

plot(t_vel_0_3mm_tube,TC_3_1)
plot(t_vel_0_3mm_tube,TC_3_4,'.')



% plot(t_vel_0_3mm_tube,V_tube,'c*')
title('Wall Temperatures')
xlabel('Time (s)')
ylabel('Temperature (°C)')
grid on
box on

axis([0 876 0 130])


legend('TC 1 4','TC 2 1','TC 2 4','TC 3 1','TC 3 4','TC 4 1','TC 4 4')

figure(4)
 hold on
plot(t_vel_0_3mm_tube,TC_Water_4)
plot(t_vel_0_3mm_tube,TC_Water_1, '.')

title('Section 1 and 4. Temperature Water')
legend('TC Water 4','TC Water 1')
xlabel('Time (s)')
ylabel('Temperature (°C)')

grid on
box on

axis([0 876 10 80])

figure(5)
 hold on
plot(t_vel_0_3mm_tube,TC_Water_ref_in)
plot(t_vel_0_3mm_tube,TC_Water_ref_out,'.')

legend('TC Water ref in','TC Water ref out')
xlabel('Time (s)')
ylabel('Temperature (°C)')
title('Refrigeration Temperature')

grid on
box on

axis([0 876 10 19])
```

```
% Sections of the tube:
x_1=0.485;
x_2=0.62;
x_3=0.69;
x_4=0.905;
h_agua=1;
h_tubo=1.5;


% Q absorbed by the refrigeration cycle

m_ref= 8.2/60;
cp=4180;
a=max(find(V_tube>0.5));
%End of the heating process
d=max(find(V_tube(1:a-1)<0.8));
%Start of the heating process

Q_ref=m_ref.*cp.*(TC_Water_ref_out(d:a)-TC_Water_ref_in(d:a));

% Q absorved by the water

%%POINT4

rho_w=1000;
%Density of water (kg/m^3)
V_w=pi*d_int^2/4*(h_agua-x_1);
%
m=rho_w*V_w;
cp=4180;
dif_T_calent_agua4=diff(T_calent_agua_4_lineal);
dif_time_calent_agua4=diff(t_calent);
slope_calent_agua4=dif_T_calent_agua4./dif_time_calent_agua4;
p=length(t_calent)-1;
Qabs_water4=m*cp*slope_calent_agua4;

% % POINT1
dif_T_calent_agua1=diff(T_calent_agua_1_lineal);
dif_time_calent_agua1=diff(t_calent);
slope_calent_agua1=dif_T_calent_agua1./dif_time_calent_agua1;
Qabs_water1=m*cp*slope_calent_agua1;

%%Mean Value

Qabs_water=(Qabs_water4+Qabs_water1)/2;

%%Q absorved by the tube



delta_a=0.004;     %thickness of the first layer (m)
rho_a=8238;      %first layer density (firebrick) (kg/m^3)
cp_a=468;          %first layer specific heat (firebrick) (J/kg*K)
k_a=13.4;            %first layer thermal conductivity
(firebrick)(W/m*K)
d_ext=0.06;
d_int=d_ext-2*delta_a;
h=h_tubo-x_1;
V=pi*(d_ext^2-d_int^2)/4*h;
```

```
m_a=V*rho_a;
dif_T_wall_calent4_1=diff(T_wall_calent_4_1_lineal);
dif_time_calent_agua4=diff(t_calent);
slope_calent_wall4_1=dif_T_wall_calent4_1./dif_time_calent_agua4;

Qabs_tube=m_a*cp_a*slope_calent_wall4_1;

 figure (12)
   hold on

   plot(t_calent(1:p),Qabs_water1)
   plot(t_calent(1:p),Qabs_tube,'c')
   plot(t_calent,Q_ref_mean,'g')
   plot(t_calent(1:p),Qabs_water4,'y')
   plot(t_calent(1:p),Qabs_water,'r')

legend('QabsWaterSection1','QabsWall','Qrefrigeration','QabsWaterSecti
on4','MeanQabsWater')
```

- This code was used for the circulation experiment.

```
clear; clc; close all
fileID = fopen('frec20Hz_v2.lvm');
T_pot_10_vel_0_30_01=textscan(fileID,'%f %f %f %f %f %f %f %f %f %f %f
%f %f %f %f %f %f %f %f %f %f %f %f %f');
fclose(fileID);

%%First we have to correlate the data saved in the file with its
correspondant thermocouple. The thermocouples that did not measure
properly were not taken into account and are shown as commented.

t_pot_10_vel_0_30_01=T_pot_10_vel_0_30_01{1};
Pressure_mA=T_pot_10_vel_0_30_01{2};
TC_press=T_pot_10_vel_0_30_01{3};
TC_1_4=T_pot_10_vel_0_30_01{4};
TC_1_1=T_pot_10_vel_0_30_01{5};
TC_2_1=T_pot_10_vel_0_30_01{6};
TC_2_2=T_pot_10_vel_0_30_01{7};
TC_2_3=T_pot_10_vel_0_30_01{8};
TC_2_4=T_pot_10_vel_0_30_01{9};
TC_2_5=T_pot_10_vel_0_30_01{10};
TC_2_6=T_pot_10_vel_0_30_01{11};
% TC_3_1=T_pot_10_vel_0_30_01{12};
TC_3_2=T_pot_10_vel_0_30_01{13};
TC_3_3=T_pot_10_vel_0_30_01{14};
TC_3_4=T_pot_10_vel_0_30_01{15};
TC_3_5=T_pot_10_vel_0_30_01{16};
TC_3_6=T_pot_10_vel_0_30_01{17};
TC_4_1=T_pot_10_vel_0_30_01{18};
TC_4_4=T_pot_10_vel_0_30_01{19};
TC_Tank_High=T_pot_10_vel_0_30_01{20};
TC_Tank_Med=T_pot_10_vel_0_30_01{21};
TC_Salt_before=T_pot_10_vel_0_30_01{22};
TC_Salt_after=T_pot_10_vel_0_30_01{23};
TC_9_Flow=T_pot_10_vel_0_30_01{24};
TC_ambientT=T_pot_10_vel_0_30_01{25};

figure(1)
hold on
plot(t_pot_10_vel_0_30_01,TC_Tank_High,'.')
plot(t_pot_10_vel_0_30_01,TC_Tank_Med,'r.')

legend('TC Tank high','TC Tank Med')

title('TANK TEMPERATURE')
xlabel('Time(s)')
ylabel('Temperature (°C)')
grid on
box on

figure(2)
hold on

plot(t_pot_10_vel_0_30_01,TC_Salt_before,'y.')
plot(t_pot_10_vel_0_30_01,TC_Salt_after,'k.')


title('SECTION 1 & 4. Temperature of the Salts')
xlabel('Time(s)')
```

```
ylabel('Temperature (°C)')
grid on
box on
axis([55 700 415 440])

legend('TC salt before','TC salt after','TC 9 flow')


figure(3)
hold on

plot(t_pot_10_vel_0_30_01,TC_2_1,'r.')
plot(t_pot_10_vel_0_30_01,TC_2_2,'k.')
plot(t_pot_10_vel_0_30_01,TC_2_3,'b*')
plot(t_pot_10_vel_0_30_01,TC_2_4,'y.')
plot(t_pot_10_vel_0_30_01,TC_2_5,'-')
plot(t_pot_10_vel_0_30_01,TC_2_6,'g.')

title('SECTION 2')
xlabel('Time(s)')
ylabel('Temperature (°C)')
grid on
box on
axis ([50 700 375 420])

legend('TC 2.1','TC 2.2','TC 2.3','TC 2.4','TC 2.5','TC 2.6')

figure(4)
hold on


plot(t_pot_10_vel_0_30_01,TC_3_2,'k.')
plot(t_pot_10_vel_0_30_01,TC_3_3,'b*')
plot(t_pot_10_vel_0_30_01,TC_3_4,'y.')
plot(t_pot_10_vel_0_30_01,TC_3_5,'-')
plot(t_pot_10_vel_0_30_01,TC_3_6,'g.')

title('SECTION 3')
xlabel('Time(s)')
ylabel('Temperature (°C)')
grid on
box on
axis ([50 730 370 420 ])

legend('TC 3.2','TC 3.3','TC 3.4','TC 3.5','TC 3.6')

figure(5)
hold on


plot(t_pot_10_vel_0_30_01,TC_1_4,'k.')
plot(t_pot_10_vel_0_30_01,TC_4_4,'b*')
plot(t_pot_10_vel_0_30_01,TC_4_1,'y.')

title('SECTION 1 & 4')
xlabel('Time(s)')
ylabel('Temperature (°C)')
grid on
box on
```

```
axis ([50 700 395 420 ])
legend('TC 1.4','TC 4.1','TC 4.4')

%Heat transfer study

a=67;
%Instant the circulation starts (s)
b=666;
%Instant the circulation stops (s)

vflow=2,24;
%velocity of the flow for the selected frequency (m/s)
Dint=0.052;
%Internal Diameter tube (m)
Dext=0.06;
%External diameter tube (m)
Aint=pi*(Dint^2)/4;
%Internal area of the tube (m^2)
Aext=pi*(Dext^2)/4;
%External area (m^2)
Tsaltafter=TC_Salt_after(a:b);
%(°C)
Tsaltbef=TC_Salt_before(a:b);
%(°C)
Tsalt=(Tsaltafter+Tsaltbef)/2;
%(°C)
Qflow=vflow*Aint;
%Volume flow rate of the salts ((m^3)/s)
Rho_salt=2090-(0.636*Tsalt);
%Density of the molten salts (kg/m^3)
mflow_salt=Qflow*Rho_salt;
%Mass flow of the salts (kg/s)
Cp_salt=1443+(0.172*Tsalt);
%Specific heat capacity (J/(kg*°C))
mu_salt=(22.714-(0.12*Tsalt)+((2.281*10^-4)*Tsalt.^2)-((1.474*10^-
7)*Tsalt.^3))*10^-3;      %Viscosity of the molten salts (Pa*s)
K_salt=0.443+(Tsalt*1.9*10^-4);
%Conductivity coefficient of the molten salts (W/(°C*m))
Ktube=21.4;
%Conductivity coefficient of the tube (W/(°C*m))
dist_befTOafter=0.42;
%Distance from the thermocouple before and after the inductor zone(m)
Q=mflow_salt.*Cp_salt.*(Tsaltbef-Tsaltafter);
%Heat calculated from section 1 to section 4(W)
Pr=mu_salt(a:b).*Cp_salt(a:b)./K_salt(a:b);
%Prandt number
Re=(mflow_salt(a:b).*Dint./(mu_salt(a:b)*Aint));
%Reynolds number
```

BIBLIOGRAPHY

[1] "Estadísticas del Sistema Eléctrico | Red Eléctrica de España." [Online]. Available: http://www.ree.es/es/estadisticas-del-sistema-electrico/3015/3001. [Accessed: 02-May-2017].

[2] R. E. D. Electrica, "E s e i," 1997.

[3] Enerdata, "Global Energy Statistical 2016," *Global Energy Statistical 2016*, 2016. [Online]. Available: https://yearbook.enerdata.net/#energy-consumption-data.html.

[4] U.S. Energy Information Administration, *International Energy Outlook 2016*, vol. 0484(2016), no. May 2016. 2016.

[5] "IEA - Technology roadmaps." [Online]. Available: https://www.iea.org/roadmaps/. [Accessed: 13-May-2017].

[6] "2015 in review | Statistical Review of World Energy | Energy economics | BP Global." [Online]. Available: http://www.bp.com/en/global/corporate/energy-economics/statistical-review-of-world-energy/2015-in-review.html. [Accessed: 13-May-2017].

[7] European Photovoltaic Industry Association, "Solar photovoltaic electricity empowering the world," *Sol. Gener. 6*, p. 100, 2011.

[8] G. H. Brundtland, "Our Common Future: Report of the World Commission on Environment and Development," *Med. Confl. Surviv.*, vol. 4, no. 1, p. 300, 1987.

[9] Intergovernmental Panel on Climate Change, "IPCC Factsheet : What is the IPCC ?," pp. 1–2, 1988.

[10] "The United Nations Framework Convention on Climate Change." [Online]. Available: http://unfccc.int/essential_background/convention/items/2627.php. [Accessed: 01-May-2017].

[11] "Kyoto Protocol 10th Anniversary - Timely Reminder Climate Agreements Work." [Online]. Available: http://newsroom.unfccc.int/unfccc-newsroom/kyoto-protocol-10th-anniversary-timely-reminder-climate-agreements-work/. [Accessed: 12-May-2017].

[12] E. Commission, "2020 climate & energy package," *2020 climate & energy package*. [Online]. Available: https://ec.europa.eu/clima/policies/strategies/2020_en#tab-0-0.

[13] "Acuerdo histórico sobre el cambio climático en París." [Online]. Available: http://newsroom.unfccc.int/es/noticias/final-cop21/. [Accessed: 01-May-2017].

[14] A. y M. A. Ministerio de Agricultura, "Objetivos de reducción de emisiones de gases de efecto invernadero.pdf." .

[15] "Data and Statistics - IRENA REsource." [Online]. Available:

http://resourceirena.irena.org/gateway/dashboard/?topic=4&subTopic=17. [Accessed: 07-May-2017].

[16] Ren21, "The First Decade: 2004-2014, 10 Years of Renewable Energy Progress," pp. 2004–2014, 2014.

[17] "CSP vs PV – Understanding the current situation and future outlook | UCL UCL Institute for Sustainable Resources Blog." [Online]. Available: https://blogs.ucl.ac.uk/sustainable-resources/2015/11/30/csp-vs-pv-understanding-the-current-situation-and-future-outlook/. [Accessed: 15-May-2017].

[18] C. S. Power, "Technology Roadmap Concentrating Solar Power," *Current*, vol. 5, pp. 1–52, 2010.

[19] International Energy Agency, "Technology Roadmap Solar photovoltaic energy," *Int. Energy Agency*, pp. 1–42, 2010.

[20] N. Corporation, "Introduction to Solar Radiation." [Online]. Available: https://www.newport.com/t/introduction-to-solar-radiation. [Accessed: 18-May-2017].

[21] "Belectric reveals battery storage facility at large-scale PV plant – pv magazine International." [Online]. Available: https://www.pv-magazine.com/2014/11/26/belectric-reveals-battery-storage-facility-at-large-scale-pv-plant_100017302/. [Accessed: 18-May-2017].

[22] "Torresol Energy - Planta termosolar Gemasolar." [Online]. Available: http://www.torresolenergy.com/TORRESOL/planta-gemasolar/es. [Accessed: 05-Jun-2017].

[23] K. Yoshikawa *et al.*, "Silicon heterojunction solar cell with interdigitated back contacts for a photoconversion efficiency over 26%," *Nat. Energy*, vol. 2, p. 17032, Mar. 2017.

[24] Dra. Ana Rosa Lagunas Alonso, "LA AUTOGENERACIÓN Y EL AUTOCONSUMO CON ENERGÍA SOLAR FOTOVOLTAICA: CONCEPTOS, TIPOLOGÍA, TENDENCIAS.," 2016, no. March.

[25] Estela, Greenpeace, and SolarPACES, "Solar Thermal Electricity - Global Outlook 2016," p. 114, 2016.

[26] V. K. Jebasingh and G. M. J. Herbert, "A review of solar parabolic trough collector," *Renew. Sustain. Energy Rev.*, vol. 54, pp. 1085–1091, 2016.

[27] P. Breeze, *Solar Power Generation*. 2014.

[28] "Concentrating Solar Power Projects - Maricopa Solar Project | Concentrating Solar Power | NREL." [Online]. Available: https://www.nrel.gov/csp/solarpaces/project_detail.cfm/projectID=58. [Accessed: 19-May-2017].

[29] "The end for dish-Stirling CSP technology? Infinia files for bankruptcy | Printing 3D Today." [Online]. Available: http://csp-world.com/news/20130929/001196/end-dish-stirling-csp-technology-infinia-files-bankruptcy. [Accessed: 19-May-2017].

[30] P. B. Hoffschmidt, "Receivers for Solar Tower Systems," 2014.

[31] Valeriano Ruiz Hernández; Manuel A. Silva Pérez; Isidoro Lillo Bravo, *La electricidad solar térmica, tan lejos, tan cerca*. 2009.

[32] NREL, "Concentrating Solar Power Projects by Status | Concentrating Solar Power | NREL." [Online]. Available: https://www.nrel.gov/csp/solarpaces/by_status.cfm. [Accessed: 02-Jun-2017].

[33] "Estudio del impacto macroeconómico de las energías renovables en españa," 2014.

[34] R. Instrument Corporation, "Type K Thermocouple." [Online]. Available: http://www.thermocoupleinfo.com/type-k-thermocouple.htm. [Accessed: 06-Jun-2017].

[35] "Thermocouple." [Online]. Available: http://www.omega.com/prodinfo/thermocouples.html. [Accessed: 01-Jun-2017].

[36] "PCI Board with Analog and thermocouple Inputs." [Online]. Available: http://es.omega.com/pptst/OMB-DAQBOARD-3000.html. [Accessed: 06-Jun-2017].

[37] C. Prieto, L. Miró, G. Peiró, E. Oró, A. Gil, and L. F. Cabeza, "Temperature distribution and heat losses in molten salts tanks for CSP plants," *Sol. Energy*, vol. 135, pp. 518–526, 2016.

[38] W. Wi-, "Suplemento al manual de usuario SUFLUXUS _ WIV4-1ES WaveInjector WI-400 FLUXUS F60x FLUXUS ADM 7x07 FLUXUS ADM 8x27," pp. 1–25, 2012.

[39] A. Gil *et al.*, "State of the art on high temperature thermal energy storage for power generation. Part 1-Concepts, materials and modellization," *Renew. Sustain. Energy Rev.*, vol. 14, no. 1, pp. 31–55, 2010.

[40] E. Tracing, S. L. C. Francia, and C. P. G. Madrid, "Sistema de Traceado Eléctrico tubería Sal fundida UC3M."

[41] B. K. Berggren, "Induction Heating: A Guide to the Process and Its Benefits."

[42] O. Lucia, P. Maussion, E. J. Dede, and J. M. Burdio, "Induction heating technology and its applications: Past developments, current technology, and future challenges," *IEEE Trans. Ind. Electron.*, vol. 61, no. 5, pp. 2509–2520, 2014.

[43] E. INDUCTION, "with TSC Heating Station Customer :," 2015.

[44] DAIKIN, "Packaged air-cooled water chillers and."

[45] A. B. Zavoico, “Solar Power Tower - Design Basis Document,” *Sandia Natl. Lab.*, no. July, p. 148, 2001.

[46] AK Steel Corporation, “Product Data Sheet: Stainless Steel 316/316L,” *AK Steel*, p. 2, 2007.

[47] “O f e r t a,” no. 190459, p. 190459, 2012.